Structural Engineering and Mechanics, *Vol. 73, No. 3 (2020) 271-286*
DOI: https://doi.org/10.12989/sem.2020.73.3.271

Generalized complex mode superposition approach for non-classically damped systems

Huating Chen[1,2a], Yanhui Liu*[1,2] and Ping Tan[1,2b]

[1] *Guangdong Provincial Key Laboratory of Earthquake Engineering and Applied Technology, Guangzhou University, Guangzhou, 510006, China*
[2] *Key Laboratory of Earthquake Resistance, Earthquake Mitigation and Structural Safety, Ministry of Education, Guangzhou University, Guangzhou, 510405, China*

(Received March 3, 2019, Revised September 28, 2019, Accepted October 5, 2019)

Abstract. Passive control technologies are commonly used in several areas to suppress structural vibrations by the addition of supplementary damping, and some modal damping may be heavy beyond critical damping even for regular structures with energy dissipation devices. The design of passive control structures is typically based on (complex) mode superposition approaches. However, the conventional mode superposition approach is predominantly applied to cases of under-critical damping. Moreover, when any modal damping ratio is equal or close to 1.0, the system becomes defective, i.e., a complete set of eigenvectors cannot be obtained such that some well-known algorithms for the quadratic eigenvalue problem are invalid. In this paper, a generalized complex mode superposition method that is suitable for under-critical, critical and over-critical damping is proposed and expressed in a unified form for structural displacement, velocity and acceleration responses. In the new method, the conventional algorithm for the eigenvalue problem is still valid, even though the system becomes defective due to critical modal damping. Based on the modal truncation error analysis, modal corrected methods for displacement and acceleration responses are developed to approximately consider the contribution of the truncated higher modes. Finally, the implementation of the proposed methods is presented through two numerical examples, and the effectiveness is investigated. The results also show that over-critically damped modes have a significant impact on structural responses. This study is a development of the original complex mode superposition method and can be applied well to dynamic analyses of non-classically damped systems.

Keywords: non-classical damping; complex mode superposition approach; critical damping; overcritical damping; modal corrected method

1. Introduction

Over-critical damping is normally considered quite unfamiliar in civil structures even if equipped with additional devices. However, it should be noted that an under- or over-critical damping entirely depends on the modal damping ratio. Damping in the fundamental mode is not very high typically, yet it is expected that in higher modes, a building experiences more flexural and shear deformation, which may contribute to higher damping. For instance, Uriz and Whittaker (2001) adopted the first-mode-based procedure (FEMA 273 1997) to retrofit a 3-story steel moment-resisting frame and increased the first modal damping ratio as high as 40% such that a substantial reduction in displacements could be obtained. Meanwhile, over-critical damping occurred in higher modes, resulting in a significant increase of floor acceleration and story shears (Occhiuzzi 2009, Suarez and Gaviria 2015). Whittle *et al.* (2012) compared the effectiveness of five commonly used viscous damper placement techniques and demonstrated that all these methods achieve over-critical damping. Moreover, the level of modal damping heavily depends on the selected optimization objective in an optimal approach of damper distribution. In the study conducted by Liu *et al.* (2005), over-critical damping occurs in the second mode when inter-story drift is considered as the optimization objective and in the third mode when the acceleration is considered as the optimization objective. On the other hand, the calculation of modal damping ratios is always based on undamped modes with ignoring the off-diagonal elements of the generalized damping matrix in the undamped mode space such that the modal damping ratio is underestimated (Zhou *et al.* 2004).

Structures with supplemental dampers are typical systems with non-classical damping, and the dynamic analysis required for the design can be usually accomplished by carrying out several cumbersome numerical integrations (Clough and Penzien 1995). A more efficient choice is the complex modal analysis (Veletsos and Ventura 1986, Singh 1980), and its primary limitation lies in the solution of a corresponding n-dimensional quadratic eigenvalue problem. Fortunately, the quadratic eigenvalue problem can be hugely deflated to an equivalent linear eigenvalue problem with small dimensions, based on the projection technology, and solved using the QZ algorithm developed by Moler and Stewart (1973).

*Corresponding author, Ph.D.
E-mail: Liuyanhui2012@163.com
[a] Ph.D.
E-mail: huntingchen@foxmail.com
[b] Ph.D.
E-mail: ptan@foxmail.com

ISSN: 1225-4568 (Print), 1598-6217 (Online)

Recently, Mentrasi (2012) introduced the homotopy analysis method to solve the quadratic eigenvalue problem directly after deflation without approximations, which can significantly increase computation efficiency. Furthermore, based on the complex mode superposition approach, many researchers comprehensively studied the response spectrum analyses for non-classically damped systems. For instance, Zhou *et al*. (2004) provided a refined complex complete quadratic combination (CCQC) rule for modal response peaks; Yu *et al*. (2005) and Yu and Zhou (2008) extended this rule to multiple-component and multiple-support excitations; Chen *et al.* (2017a) added the contribution of truncated higher modes. At present, dynamic analyses of non-classical damping systems can be conducted well in practice. However, the contribution of over-critically damped modes is always neglected for the convenient application of the complex mode superposition method, potentially resulting in significant errors (Takewaki 2004). Even though Chu *et al.* (2009) considered the contribution of the over-critically damped modes to the structural response, under- and over-critically damped modes cannot be unified well in the aforementioned method. Liu *et al*. (2016) proved that the present complex mode superposition method was suitable for the over-critically damped modes but a slight revision required. In addition, some modes may have critical damping, and the contribution of these modes must be taken into consideration as well. However, few researchers have addressed this issue.

It is often difficult, and even unnecessary, to obtain all the eigenpairs of a large-scale model, implying that the modal truncation scheme is generally used, and the modal truncation error is therefore introduced. As a result, the quality of the calculated structural response may be adversely affected. The corrections to the modal truncation scheme of the (real or complex) mode superposition method have been investigated by several researchers. Static correction methods or mode acceleration methods (MAMs) (Maddox 1975, Hansteen and Bell 1979, Cornwell *et al*. 1983) approximate the contribution of (unavailable) higher modes to dynamic responses in terms of a pseudo-static term. Since MAMs neglect the contribution of both velocity and acceleration terms to dynamic responses, they can be considered as state approximation methods. Traill-Nash (1981) and Singh and McCown (1986) proposed MAMs for non-classically damped systems respectively. However, the former is only suitable for the loading with analytical law, and the latter requires complex operations. These methods have been applied widely in response spectrum analyses (Singh and McCown 1986, Der Kiureghian and Nakamura 1993, Dhileep and Bose 2008) and random vibration studies (Cacciola *et al.* 2007, Benfratello and Muscolino 2001). Dynamic correction methods or modal truncation augmentation methods (MTAMs) (Dickens and Pool 1992, Dickens *et al.* 1997, Besselink *et al.* 2013), which were developed to improve the accuracy of the MAMs, include the contribution of higher modes by the particular solution of reduced differential equations of motion. Force derivative methods (FDMs) (Camarda *et al.* 1987, Akgu 1993) reduce the modal truncation error by considering the higher-order derivatives of the forcing function, implying that the forcing function should be described by analytical laws. Hybrid expansion methods (HEMs) (Liu *et al.* 1996, Huang *et al.* 1997, Li *et al.* 2014, Li *et al.* 2013, Qu 2000, Qu and Selvam 2000, Xiao *et al.* 2017) are another type of correction schemes that combine the mode superposition of the (available) lower modes with a power-series expansion of dynamic responses in terms of system matrices, which are applied widely in the frequency-domain analysis. It is important to highlight that all the aforementioned correction methods are suitable for under-critically damped systems and need to be developed further for the dynamic analysis of passive control structures due to heavy damping in some modes.

The objective of this study is to address the critical damping issue in dynamic analyses and develop a generalized dynamic analysis method based on complex modes. Due to defectiveness of system resulting from critical modal damping, the calculation of the generalized eigenvectors and the orthogonal conditions are introduced firstly in Section 2. Then, a generalized complex mode superposition method is developed in Section 3, which is expressed in a unified form without the limit of modal damping. In practice, the modal truncation scheme is always used to reduce large computation. In Section 4, the modal truncation error of the proposed complex mode superposition method is examined. Based on this error, correction methods for structural displacement and acceleration responses are developed in Section 5. Finally, two numerical examples is used to demonstrate the effectiveness of the analysis method proposed in this paper.

2. Basic equations

Consider a linear and non-classically damped structure with n degrees of freedom (DOFs). When the system is subjected to a loading $\mathbf{f}(t)$, the well-known equation of motion is

$$\mathbf{M}\ddot{\mathbf{u}} + \mathbf{C}\dot{\mathbf{u}} + \mathbf{K}\mathbf{u} = \mathbf{f}(t) \equiv \mathbf{s}f(t) \tag{1}$$

in which, $\mathbf{M}$, $\mathbf{C}$ and $\mathbf{K}$ are the symmetric mass, damping and stiffness matrices of size $n\times n$, respectively. Here, $\mathbf{M}$ and $\mathbf{K}$ are particularly restricted to positive definite, while $\mathbf{C}$ is positive semi-definite due to the non-classical damping such that the conventional mode superposition method becomes invalid. $\ddot{\mathbf{u}}$, $\dot{\mathbf{u}}$ and $\mathbf{u}$ are respectively the time-dependent acceleration, velocity and displacement vectors relative to the ground. $\mathbf{s}$ denotes the spatial distribution of the loading.

To decouple Eq. (1), it is necessary to transform the n second-order differential equations to $2n$ first-order ones, namely,

$$\mathbf{A}\dot{\mathbf{v}} + \mathbf{B}\mathbf{v} = \mathbf{\Gamma} f(t) \tag{2}$$

which is normally named as state equation. The state variable $\mathbf{v}$, the coefficient matrices $\mathbf{A}$ and $\mathbf{B}$, and the influence vector in state space $\mathbf{\Gamma}$ are

$$\mathbf{v} = \begin{Bmatrix} \dot{\mathbf{u}} \\ \mathbf{u} \end{Bmatrix} \quad \mathbf{A} = \begin{bmatrix} \mathbf{0} & \mathbf{M} \\ \mathbf{M} & \mathbf{C} \end{bmatrix} \quad \mathbf{B} = \begin{bmatrix} -\mathbf{M} & \\ & \mathbf{K} \end{bmatrix} \quad \mathbf{\Gamma} = \begin{Bmatrix} \mathbf{0} \\ \mathbf{s} \end{Bmatrix}$$

By setting the right hand side of Eq. (2) to zero, the corresponding eigenvalue problem can be obtained as

$$\mathbf{B}\boldsymbol{\psi}_i = -\lambda_i \mathbf{A}\boldsymbol{\psi}_i \tag{3}$$

It should be noted that neither of $\mathbf{A}$ and $\mathbf{B}$ is positive definite, although they are symmetric and invertible. According to the linear algebra theory, the eigenvalue λ_i and the relevant eigenvector $\boldsymbol{\psi}_i$ are, in general, complex-valued and occur in conjugate pairs when the amount of damping in the system is not very high, otherwise, they are real-valued but appear in pairs as well. To describe the vibration behavior of structure, dived the eigenvector into two parts, i.e., $\boldsymbol{\psi}_i = [\boldsymbol{\chi}_i^{\mathrm{T}}, \boldsymbol{\phi}_i^{\mathrm{T}}]^{\mathrm{T}}$, where $\boldsymbol{\chi}_i$ and $\boldsymbol{\phi}_i$ respectively represent the first and last *n* elements of $\boldsymbol{\psi}_i$. $\boldsymbol{\chi}_i$ is associated with the structural velocity and the relation $\boldsymbol{\chi}_i = \lambda_i \boldsymbol{\phi}_i$ always holds in the cases of under-critical and over-critical modal damping. $\boldsymbol{\phi}_i$ reflects the structural deformation**,** which is called complex mode in this study.

Referring to the case with classical damping, a pair of eigenvalue (λ_i, λ_i^*) can be expressed in terms of natural frequency ω_i and modal damping ratio ξ_i as

$$\lambda_i, \lambda_i^* = -\xi_i \omega_i \pm \omega_i \sqrt{\xi_i^2 - 1} \tag{4}$$

From Eq. (4), it is apparent that the forms of λ_i and λ_i^* depend directly upon the amount of ξ_i: (1) when $\xi_i < 1$, $\lambda_i, \lambda_i^* = -\xi_i \omega_i \pm \mathrm{i}\omega_i \sqrt{1 - \xi_i^2}$, where $\mathrm{i} = \sqrt{-1}$, in such case both (λ_i, λ_i^*) and $(\boldsymbol{\psi}_i, \boldsymbol{\psi}_i^*)$ are complex conjugate pairs; (2) when $\xi_i = 1$, $\lambda_i = \lambda_i^* = -\omega_i$, $(\boldsymbol{\psi}_i, \boldsymbol{\psi}_i^*)$ are real-valued. Note that the eigenvalue is repeated and the system may be defective (Friswell *et al*. 2005, Yu *et al*. 2012), which will be discussed in detail in the following section; (3) when $\xi_i > 1$, $\lambda_i, \lambda_i^* = -\xi_i \omega_i \pm \omega_i \sqrt{\xi_i^2 - 1}$, both (λ_i, λ_i^*) and $(\boldsymbol{\psi}_i, \boldsymbol{\psi}_i^*)$ are real-valued pairs.

However, the conventional complex mode superposition method is based on under-critical modal damping. As the damping increases, some eigenvalues and eigenvectors may become real-valued and this is very possible in a structure with dampers. It is necessary to improve the method to be suitable for different damping levels. The key step in carrying out the complex mode superposition method is to solve a corresponding eigenvalue problem. Therefore, the calculation and orthogonality condition of eigenvectors, especially eigenvectors with respect to the repeated eigenvalue, are first presented in the following section.

3. Eigenvalue problem with multiple modal damping levels

3.1 Usual eigenvectors and generalized eigenvectors

As a modal damping ratio increases to a value very close to 1, the imaginary parts in the pair of eigenvalues presented in Eq. (4) constantly decreases to a value very close to 0 such that the eigenvalues almost become real-valued and repeated, namely,

$$\lim_{\xi_i \to 1} \lambda_i = \lim_{\xi_i \to 1} \lambda_i^* = -\omega_i$$

In the associated pair of eigenvectors, $\boldsymbol{\phi}_i = \boldsymbol{\sigma}_i + \mathrm{i}\boldsymbol{\tau}_i$ and $\boldsymbol{\phi}_i^* = \boldsymbol{\sigma}_i - \mathrm{i}\boldsymbol{\tau}_i$, where $\boldsymbol{\sigma}_i$ and $\boldsymbol{\tau}_i$ are real-valued vectors. Similarly,

$$\lim_{\xi_i \to 1} \boldsymbol{\phi}_i = \lim_{\xi_i \to 1} \boldsymbol{\phi}_i^* = \boldsymbol{\sigma}_i$$

Hence, it can be concluded that the pair of eigenvectors will become linear dependent with the modal damping ratio being equal or close to 1 due to the existence of computer rounding errors in practice. In other words, $\mathbf{A}$ and $\mathbf{B}$ become defective such that the independent eigenvectors for the repeated eigenvalues cannot be obtained using the QZ algorithm alone without the special process. Due to the loss of one eigenvector, the obtained eigenvectors cannot span a complete space. As a result, the structural response in the space cannot be expressed in terms of these eigenvectors.

In tandem with the argument presented above, a non-classically damped system with critical modal damping must be defective. Under this circumstance, $\mathbf{A}$ and $\mathbf{B}$ cannot be diagonalized simultaneously, and the complex superposition method becomes invalid. Transforming the generalized eigenvalue problem, Eq. (3), into a normalized one, $\mathbf{D}\boldsymbol{\psi}_i = -\lambda_i \boldsymbol{\psi}_i$, where $\mathbf{D} = \mathbf{A}^{-1}\mathbf{B}$ is more convenient to study for a defective system. According to the linear algebra theory, eigenvalue decomposition may not exist for one matrix, but the Jordan decomposition always exists. Therefore,

$$\mathbf{D} = \boldsymbol{\Psi}\mathbf{J}\boldsymbol{\Psi}^{-1} \tag{5}$$

wherein $\boldsymbol{\Psi}$ denotes the invertible transform matrix, and $\mathbf{J}$ is the so-called Jordan matrix, which is a nearly diagonal matrix with eigenvalues along its principal diagonal and a number of unit elements in its super-diagonal line.

Supposing that one eigenvalue, λ_r, occurs twice due to critical modal damping, i.e., $\lambda_r = \lambda_r^*$, $\mathbf{J}$ has the following form,

$$\mathbf{J} = \begin{bmatrix} \lambda_1 & & & & & & & \\ & \lambda_1^* & & & & & & \\ & & \ddots & & & & & \\ & & & \lambda_r & 1 & & & \\ & & & & \lambda_r & & & \\ & & & & & \ddots & & \\ & & & & & & \lambda_n & \\ & & & & & & & \lambda_n^* \end{bmatrix}$$

Pre-multiplying Eq. (5) by $\mathbf{A}$ and post-multiplying it by $\boldsymbol{\Psi}$ leads to,

$$\mathbf{B}\boldsymbol{\Psi} = -\mathbf{A}\,\boldsymbol{\Psi}\mathbf{J} \tag{6}$$

If the columns of $\boldsymbol{\Psi}$ are called $\boldsymbol{\psi}_1 \quad \boldsymbol{\psi}_1^* \quad \cdots \quad \boldsymbol{\psi}_r \quad \boldsymbol{\psi}_r^* \quad \cdots \quad \boldsymbol{\psi}_n \quad \boldsymbol{\psi}_n^*$, the *j*-th ($j \neq r$) pair of columns on both sides of Eq. (6) yields,

$$\mathbf{B}\boldsymbol{\psi}_j = -\lambda_j \mathbf{A}\boldsymbol{\psi}_j \tag{7.a}$$

$$\mathbf{B}\boldsymbol{\psi}_j^* = -\lambda_j^* \mathbf{A}\boldsymbol{\psi}_j^* \tag{7.b}$$

confirming that $\boldsymbol{\psi}_j$ and $\boldsymbol{\psi}_j^*$ are the usual eigenvectors of $\mathbf{A}$ and $\mathbf{B}$ (for under-critical modal damping, "*" denotes a complex conjugate, and for overcritical modal damping, both are real-valued). Similarly, the *r*-th pair of columns on both sides of Eq. (6) result in,

$$\mathbf{B}\boldsymbol{\psi}_r = -\lambda_r \mathbf{A}\boldsymbol{\psi}_r \tag{8.a}$$

$$(\mathbf{B} + \lambda_r \mathbf{A})\boldsymbol{\psi}_r^* = -\mathbf{A}\boldsymbol{\psi}_r \tag{8.b}$$

Therefore, it is evident that $\boldsymbol{\psi}_r^*$ is not an eigenvector, because it does not satisfy an equation such as Eq. (7). Instead, in this paper, $\boldsymbol{\psi}_r^*$ represents a generalized eigenvector of **A** and **B**. In practice, eigenvalues are typically obtained prior to eigenvectors using the QZ algorithm. The corresponding eigenvectors can then be calculated using back-substitution processes. However, a generalized eigenvector can only be obtained from Eq. (8.b) after $\boldsymbol{\psi}_r$ is known. Using the definition of linear independence of vectors and considering Eq. (8), it can be easily proved that $\boldsymbol{\psi}_r$ and $\boldsymbol{\psi}_r^*$ are linearly independent. Furthermore, all the usual and generalized eigenvectors are linearly independent as well, which can be proved using the orthogonality conditions in the following section. These vectors can then be used as a complete set of bases for the $2n$-dementional space.

3.2 Orthogonality conditions

It can be proved that different usual eigenvectors (including $\boldsymbol{\psi}_r$), regardless of whether they correspond to under- and over-critical modal damping have orthogonality conditions with respect to **A** and **B**, namely,

$$\boldsymbol{\psi}_i^{\mathrm{T}}\mathbf{A}\boldsymbol{\psi}_j = 0 \qquad \boldsymbol{\psi}_i^{\mathrm{T}}\mathbf{B}\boldsymbol{\psi}_j = 0 \qquad i \neq j \tag{9.a}$$

$$(\boldsymbol{\psi}_i^*)^{\mathrm{T}}\mathbf{A}\boldsymbol{\psi}_j = 0 \quad (\boldsymbol{\psi}_i^*)^{\mathrm{T}}\mathbf{B}\boldsymbol{\psi}_j = 0 \quad i \neq r \tag{9.b}$$

$$(\boldsymbol{\psi}_i^*)^{\mathrm{T}}\mathbf{A}\boldsymbol{\psi}_j^* = 0 \quad (\boldsymbol{\psi}_i^*)^{\mathrm{T}}\mathbf{B}\boldsymbol{\psi}_j^* = 0 \quad i,j \neq r, i \neq j \tag{9.c}$$

Similarly, the generalized eigenvector, $\boldsymbol{\psi}_r^*$, and other usual eigenvectors such as $\boldsymbol{\psi}_j$ and $\boldsymbol{\psi}_j^*$ satisfy the following conditions due to the difference in their eigenvalues,

$$(\boldsymbol{\psi}_r^*)^{\mathrm{T}}\mathbf{A}\boldsymbol{\psi}_j = 0 \quad (\boldsymbol{\psi}_r^*)^{\mathrm{T}}\mathbf{B}\boldsymbol{\psi}_j = 0 \quad j \neq r \tag{10.a}$$

$$(\boldsymbol{\psi}_r^*)^{\mathrm{T}}\mathbf{A}\boldsymbol{\psi}_j^* = 0 \quad (\boldsymbol{\psi}_r^*)^{\mathrm{T}}\mathbf{B}\boldsymbol{\psi}_j^* = 0 \quad j \neq r \tag{10.b}$$

In this study, we are concerned with the relationship between $\boldsymbol{\psi}_r$ and $\boldsymbol{\psi}_r^*$. Pre-multiplying Eq. (8.a) by $(\boldsymbol{\psi}_r^*)^{\mathrm{T}}$ and Eq. (8.b) by $\boldsymbol{\psi}_r^{\mathrm{T}}$ leads to,

$$(\boldsymbol{\psi}_r^*)^{\mathrm{T}}\mathbf{B}\boldsymbol{\psi}_r = -\lambda_r(\boldsymbol{\psi}_r^*)^{\mathrm{T}}\mathbf{A}\boldsymbol{\psi}_r \tag{11.a}$$

$$\boldsymbol{\psi}_r^{\mathrm{T}}\mathbf{B}\boldsymbol{\psi}_r^* = -\boldsymbol{\psi}_r^{\mathrm{T}}\mathbf{A}\boldsymbol{\psi}_r - \lambda_r\boldsymbol{\psi}_r^{\mathrm{T}}\mathbf{A}\boldsymbol{\psi}_r^* \tag{11.b}$$

Taking account of the symmetry of **A** and **B**, the above equations yield,

$$\boldsymbol{\psi}_r^{\mathrm{T}}\mathbf{A}\boldsymbol{\psi}_r = \boldsymbol{\psi}_r^{\mathrm{T}}\mathbf{B}\boldsymbol{\psi}_r = 0 \tag{12.a}$$

$$\boldsymbol{\psi}_r^{\mathrm{T}}\mathbf{A}\boldsymbol{\psi}_r^* \neq 0 \qquad \boldsymbol{\psi}_r^{\mathrm{T}}\mathbf{B}\boldsymbol{\psi}_r^* \neq 0 \tag{12.b}$$

Therefore, $\boldsymbol{\psi}_r$ and $\boldsymbol{\psi}_r^*$ do not have the orthogonality condition like the other eigenvectors. In addition, the above conditions differ from those in a non-defective system with independent eigenvectors for a repeated eigenvalue wherein,

$$\boldsymbol{\psi}_r^{\mathrm{T}}\mathbf{A}\boldsymbol{\psi}_r \neq 0 \qquad \boldsymbol{\psi}_r^{\mathrm{T}}\mathbf{B}\boldsymbol{\psi}_r \neq 0 \tag{13.a}$$

$$\boldsymbol{\psi}_r^{\mathrm{T}}\mathbf{A}\boldsymbol{\psi}_r^* = \boldsymbol{\psi}_r^{\mathrm{T}}\mathbf{B}\boldsymbol{\psi}_r^* = 0 \tag{13.b}$$

4. Generalized complex mode superposition approach

As well known, for under-critical modal damping, eigensolutions appear in the form of complex conjugate pairs, whereas for over-critical modal damping, they are real-valued and appear in pairs. However, **A** and **B** cannot be diagonalized simultaneously for critical modal damping from Eq. (12).

Suppose that the damping of the system is high such that under-critical, critical and over-critical modal damping exist simultaneously. In this case, the system is defective, and only the Jordan decomposition can be conducted. Even though no orthogonality condition exists for $\boldsymbol{\psi}_r^*$ and $\boldsymbol{\psi}_r$, they are linearly independent. Therefore, all the usual and generalized eigenvectors can construct a complete set of bases for the $2n$-dimensional space corresponding to **A** and **B** such that the state vector **v** in the space can be expressed in terms of these bases as,

$$\mathbf{v}(t) = \boldsymbol{\Psi}\mathbf{z}(t) \tag{14}$$

wherein $\mathbf{z}(t) = [z_1 \quad z_1^* \quad \cdots \quad z_r \quad z_r^* \quad \cdots \quad z_n \quad z_n^*]^{\mathrm{T}}$ is a generalized coordinate vector.

Substituting Eq. (14) into Eq. (2), pre-multiplying by $\boldsymbol{\Psi}^{\mathrm{T}}$ and considering the conditions shown in Eqs. (9), (10) and (12) yields,

$$\mathbf{a}\,\dot{\mathbf{z}}(t) + \mathbf{b}\,\mathbf{z}(t) = \boldsymbol{\theta}f(t) \tag{15}$$

wherein $\boldsymbol{\theta} = \boldsymbol{\Psi}^{\mathrm{T}}\boldsymbol{\Gamma} = [\theta_1 \quad \theta_1^* \quad \cdots \quad \theta_r \quad \theta_r^* \quad \cdots \quad \theta_n \quad \theta_n^*]^{\mathrm{T}}$ and $\theta_i = \boldsymbol{\psi}_i^{\mathrm{T}}\boldsymbol{\Gamma}$, $\theta_i^* = (\boldsymbol{\psi}_i^*)^{\mathrm{T}}\boldsymbol{\Gamma}$ (including $i = r$). Coefficient matrices **a** and **b** have the following forms,

$$\mathbf{a} = \begin{bmatrix} a_1 & & & & & & & \\ & a_1^* & & & & & & \\ & & \ddots & & & & & \\ & & & 0 & \alpha_r & & & \\ & & & \alpha_r & a_r^* & & & \\ & & & & & \ddots & & \\ & & & & & & a_n & \\ & & & & & & & a_n^* \end{bmatrix}$$

$$\mathbf{b} = \begin{bmatrix} b_1 & & & & & & & \\ & b_1^* & & & & & & \\ & & \ddots & & & & & \\ & & & 0 & \beta_r & & & \\ & & & \beta_r & b_r^* & & & \\ & & & & & \ddots & & \\ & & & & & & b_n & \\ & & & & & & & b_n^* \end{bmatrix}$$

wherein $a_i = \boldsymbol{\psi}_i^{\mathrm{T}}\mathbf{A}\boldsymbol{\psi}_i$, $a_i^* = (\boldsymbol{\psi}_i^*)^{\mathrm{T}}\mathbf{A}\boldsymbol{\psi}_i^*$, $b_i = \boldsymbol{\psi}_i^{\mathrm{T}}\mathbf{B}\boldsymbol{\psi}_i$, $b_i^* = (\boldsymbol{\psi}_i^*)^{\mathrm{T}}\mathbf{B}\boldsymbol{\psi}_i^*$, $\alpha_r = \boldsymbol{\psi}_r^{\mathrm{T}}\mathbf{A}\boldsymbol{\psi}_r^*$ and $\beta_r = \boldsymbol{\psi}_r^{\mathrm{T}}\mathbf{B}\boldsymbol{\psi}_r^*$.

The elements of the matrices and vectors in Eq. (15) are complex-valued or real-valued depending on the associated modal damping. Moreover, the r-th pair of modal equations of motion are evidently coupled. Therefore, the modal equations of motion with under-critical, critical and overcritical modal damping are addressed individually in the consequent sections.

4.1 Under-critical modal damping

For the modes with under-critical damping, the modal equations of motion occur in complex conjugate pairs. From Eq. (15), the i-th pair of modal equations of motion corresponding to under-critical modal damping are,

$$\dot{z}_i(t) - \lambda_i z_i(t) = \eta_i f(t) \tag{16.a}$$

$$\dot{\bar{z}}_i(t) - \bar{\lambda}_i \bar{z}_i(t) = \bar{\eta}_i f(t) \tag{16.b}$$

wherein the superposed bar denotes the complex conjugate; $\eta_i = \theta_i / a_i$ and $\bar{\eta}_i = \bar{\theta}_i / \bar{a}_i$ are the i-th pair of modal participation factors. Eq. (16) is a set of first-order differential equations that can be solved easily using classical mathematical methods. However, it is more useful to associate $z_i(t)$ with the equation of motion for a normalized SDOF system,

$$\ddot{q}_i(t) + 2\xi_i \omega_i \dot{q}_i(t) + \omega_i^2 q_i(t) = f(t) \tag{17}$$

Recalling the derivative of the Duhamel integration (Chen *et al.* 2017b), $z_i(t)$ can be expressed by $q_i(t)$ and $\dot{q}_i(t)$ as,

$$z_i(t) = \eta_i[\dot{q}_i(t) + (\xi_i\omega_i + \mathrm{i}\omega_{Di})q_i(t)] \tag{18}$$

The structural displacement corresponding to the i-th pair of complex conjugate eigenvectors is given by,

$$\mathbf{u}_i(t) = \boldsymbol{\phi}_i z_i(t) + \bar{\boldsymbol{\phi}}_i \bar{z}_i(t) = \boldsymbol{\rho}_i^d \dot{q}_i(t) + \boldsymbol{\varphi}_i^d q_i(t) \tag{19}$$

wherein $\boldsymbol{\rho}_i^d = 2\mathrm{Re}(\boldsymbol{\phi}_i \eta_i)$ and $\boldsymbol{\varphi}_i^d = -2\mathrm{Re}(\bar{\lambda}_i \boldsymbol{\phi}_i \eta_i)$ with $\mathrm{Re}(\cdot)$ denoting the real part of a complex value. The modal responses $q_i(t)$ and $\dot{q}_i(t)$ can be calculated using many well-known numerical methods in the time domain. If all modal damping is under-critical, the conventional complex mode superposition method can be obtained by combining all the displacement responses represented by Eq. (19).

4.2 Critical modal damping

Pre-multiplying Eq. (8.b) by $(\boldsymbol{\psi}_r^*)^{\mathrm{T}}$ and considering Eq. (11) yields the following relations,

$$b_r^* + \lambda_r a_r^* = -\alpha_r \qquad \beta_r = -\lambda_r \alpha_r \tag{20}$$

For the critical damping mode, the associated modal equations of motion can be expressed from Eq. (15) as,

$$\dot{z}_r - \lambda_r z_r = z_r^* + \eta_r f(t) \tag{21.a}$$

$$\dot{z}_r^* - \lambda_r z_r^* = \eta_r^* f(t) \tag{21.b}$$

wherein η_r and η_r^* are the r-th pair of modal participation coefficients for the critical damping mode, namely,

$$\eta_r = \frac{(\boldsymbol{\psi}_r^* - a_r^*/\alpha_r \boldsymbol{\psi}_r)^{\mathrm{T}}\boldsymbol{\Gamma}}{\alpha_r} \qquad \eta_r^* = \frac{\boldsymbol{\psi}_r^{\mathrm{T}}\boldsymbol{\Gamma}}{\alpha_r}$$

Eq. (21) is coupled, which is very different from the normal modal equations of motion in Eq. (16). Considering the superposition principle of solutions for a linear differential equation, the unknown z_r in Eq. (21.a) can be divided into two components,

$$z_r = z_r^{(1)} + z_r^{(2)} \tag{22}$$

wherein $z_r^{(1)}$ and $z_r^{(2)}$ are solutions to,

$$\dot{z}_r^{(1)} - \lambda_r z_r^{(1)} = z_r^* \tag{23}$$

$$\dot{z}_r^{(2)} - \lambda_r z_r^{(2)} = \eta_r f(t) \tag{24}$$

respectively. Differentiating Eq. (23) with respect to time t using Eqs. (21.b) and (23) yields,

$$\ddot{z}_r^{(1)} - 2\lambda_r \dot{z}_r^{(1)} + \lambda_r^2 z_r^{(1)} = \eta_r^* f(t) \tag{25}$$

The solutions of Eqs. (24) and (25) can be obtained through Laplace integral transformation,

$$\begin{cases} z_r^{(1)} = \eta_r^* \displaystyle\int_0^t f(\tau)(t-\tau)\exp[\lambda_r(t-\tau)]\mathrm{d}\tau \\ z_r^{(2)} = \eta_r \displaystyle\int_0^t f(\tau)\exp[\lambda_r(t-\tau)]\mathrm{d}\tau \end{cases} \tag{26}$$

Introducing the Duhamel integration of a critically-damped SDOF system represented by Eq. (17) and its derivative into Eq. (26) or utilizing the Laplace transformation directly yields,

$$\begin{cases} z_r = (\eta_r^* + \omega_r \eta_r) q_r(t) + \eta_r \dot{q}_r(t) \\ z_r^* = \eta_r^*[\omega_r q_r(t) + \dot{q}_r(t)] \end{cases} \tag{27}$$

wherein $q_r(t)$ and $\dot{q}_r(t)$ denote displacement and velocity respectively of the SDOF system with respect to critical damping. The expressions of z_r and z_r^* above are evidently independent such that the displacement responses corresponding to the usual and generalized eigenvector can be given by,

$$\mathbf{u}_r(t) = \boldsymbol{\phi}_r z_r(t) + \boldsymbol{\phi}_r^* z_r^*(t) = \boldsymbol{\rho}_r^d \dot{q}_r(t) + \boldsymbol{\varphi}_r^d q_r(t) \tag{28}$$

wherein $\boldsymbol{\rho}_r^d = \eta_r \boldsymbol{\phi}_r + \eta_r^* \boldsymbol{\phi}_r^*$ and $\boldsymbol{\varphi}_r^d = (\eta_r^* - \lambda_r \eta_r)\boldsymbol{\phi}_r - \lambda_r \eta_r^* \boldsymbol{\phi}_r^*$. Here, $\boldsymbol{\phi}_r$ and $\boldsymbol{\phi}_r^*$ are the second n elements of $\boldsymbol{\psi}_r$ and $\boldsymbol{\psi}_r^*$ respectively, and $\boldsymbol{\phi}_r^*$ can be called the generalized mode vector.

4.3 Over-critical modal damping

For over-critically damped eigenvectors, both the modes and the corresponding eigenvalues are real-valued and appear in pairs—$(\boldsymbol{\phi}_j, \hat{\boldsymbol{\phi}}_j)$ and $(\lambda_j, \hat{\lambda}_j)$. Based on the orthogonalization conditions in Section 3, the decoupled modal equations of motion relevant to a pair of over-critically damped eigenvectors are,

$$\begin{cases} \dot{z}_j - \lambda_j z_j = \eta_j f(t) \\ \dot{\hat{z}}_j - \hat{\lambda}_j \hat{z}_j = \hat{\eta}_j f(t) \end{cases} \tag{29}$$

wherein z_j and $\hat{z}_j$ are a pair of real-valued generalized coordinates. $\eta_j = \theta_j / a_j$ and $\hat{\eta}_j = \hat{\theta}_j / \hat{a}_j$ are the j-th pair of modal participation factors, and they are real-valued. In addition, for the over-critically damped mode, $\lambda_j, \hat{\lambda}_j =$

$-\xi_j\omega_j \pm \widehat{\omega}_{Dj}$, wherein $\widehat{\omega}_{Dj} = \omega_j\sqrt{\xi_j^2 - 1}$ and $\xi_j > 1$. Eq. (29) is a set of first-order linear ordinary differential equations, and their solutions can be obtained easily,

$$\begin{cases} z_j = \eta_j \int_0^t f(\tau)\exp\left[\lambda_j(t-\tau)\right]\mathrm{d}\tau \\ \hat{z}_j = \hat{\eta}_j \int_0^t f(\tau)\exp\left[\hat{\lambda}_j(t-\tau)\right]\mathrm{d}\tau \end{cases} \tag{30}$$

Similarly, introducing the Duhamel integration of an over-critically damped SDOF system is represented by Eq. (17) and its derivative, Eq. (29) can be rewritten as,

$$\begin{cases} z_j = \eta_j\left[\dot{q}_j(t) + \left(\xi_j\omega_j + \widehat{\omega}_{Dj}\right)q_j(t)\right] \\ \hat{z}_j = \hat{\eta}_j\left[\dot{q}_j(t) + \left(\xi_j\omega_j - \widehat{\omega}_{Dj}\right)q_j(t)\right] \end{cases} \tag{31}$$

Finally, the displacement response corresponding to a pair of over-critically damped mode vectors can be given by,

$$\mathbf{u}_j(t) = \boldsymbol{\Phi}_j z_j(t) + \widehat{\boldsymbol{\Phi}}_j \hat{z}_j(t) = \boldsymbol{\rho}_j^d \dot{q}_j(t) + \boldsymbol{\varphi}_j^d q_j(t) \tag{32}$$

wherein $\boldsymbol{\rho}_j^d = \eta_j\boldsymbol{\Phi}_j + \hat{\eta}_j\widehat{\boldsymbol{\Phi}}_j$ and $\boldsymbol{\varphi}_j^d = -\hat{\lambda}_j\eta_j\boldsymbol{\Phi}_j - \lambda_j\hat{\eta}_j\widehat{\boldsymbol{\Phi}}_j$. Chu *et al.* (2009) provided an expression for over-critically damped responses. However, in their study, all the over-critically damped modes were handled individually instead of being grouped in pairs as shown in Eqs. (29) and (32), which is useful to derive a unified form for the improved complex modal superposition method, as shown in the consequent section.

4.4 Structural responses

Based on the preceding discussions, we can conclude that the same expression for the displacement response exist for different modal damping levels represented by a pair of mode vectors. Therefore, regardless of the damping level of the non-classically damped system, the total structural displacement can be obtained by combining all the modal displacements from Eqs. (19), (28) and (32), namely,

$$\mathbf{u}(t) = \sum_{i=1}^{n}\left[\boldsymbol{\rho}_i^d \dot{q}_i(t) + \boldsymbol{\varphi}_i^d q_i(t)\right] \tag{33}$$

However, it should be noted that the calculations for the coefficient vectors $\boldsymbol{\rho}_i^d$ and $\boldsymbol{\varphi}_i^d$ differ depending upon the modal damping ratio, and they are summarized as follows,

$$\begin{cases} \boldsymbol{\rho}_i^d = \eta_i\boldsymbol{\Phi}_i + \eta_i^*\boldsymbol{\Phi}_i^*, \boldsymbol{\varphi}_i^d = -\lambda_i^*\eta_i\boldsymbol{\Phi}_i - \lambda_i\eta_i^*\boldsymbol{\Phi}_i^* & \xi_i \neq 1 \\ \boldsymbol{\rho}_i^d = \eta_i\boldsymbol{\Phi}_i + \eta_i^*\boldsymbol{\Phi}_i^*, \boldsymbol{\varphi}_i^d = (\eta_i^* - \lambda_i\eta_i)\boldsymbol{\Phi}_i - \lambda_i\eta_i^*\boldsymbol{\Phi}_i^* & \xi_i = 1 \end{cases}$$

Since $\xi_i \neq 1$, including two cases, i.e., under- and over-critical modal damping, $\boldsymbol{\Phi}_i$ and $\boldsymbol{\Phi}_i^*$ are a usual mode pair obtained directly from eigensolutions, and the modal participation coefficients are given by uniform expressions, $\eta_i = \theta_i/a_i$ and $\eta_i^* = \theta_i^*/a_i^*$. In case $\xi_i = 1$, $\boldsymbol{\Phi}_i^*$ is a generalized mode calculated by Eq. (8.b) after the usual mode $\boldsymbol{\Phi}_i$ has been obtained, and the associated modal participation coefficients need to be calculated particularly using the expressions presented in Section 4.2.

Intuitively, the structural velocity responses can be obtained directly by using the derivative of Eq. (33) with respect to the time variable *t*. This approach appears simple and has been used by researchers such as Takewaki (2004). However, the formulation requires the incorporation of an additional modal response $\ddot{q}_i(t)$ in the expression. A simpler expression for the structural velocity response can be derived by considering Eq. (17) after using the time derivative of Eq. (33), which can be expressed as,

$$\dot{\mathbf{u}}(t) = \sum_{i=1}^{n}\left[\boldsymbol{\rho}_i^v \dot{q}_i(t) + \boldsymbol{\varphi}_i^v q_i(t)\right] \tag{34}$$

wherein $\boldsymbol{\rho}_i^v = \boldsymbol{\varphi}_i^d - 2\xi_i\omega_i\boldsymbol{\rho}_i^d$ and $\boldsymbol{\varphi}_i^v = -\omega_i^2\boldsymbol{\rho}_i^d$. In addition, in the above derivation, another relation, $\sum_{i=1}^{n}\boldsymbol{\rho}_i^d = \sum_{i=1}^{n}(\eta_i\boldsymbol{\Phi}_i + \eta_i^*\boldsymbol{\Phi}_i^*) = \mathbf{0}$, is used, and this relation can be proved easily,

$$\mathbf{A}^{-1}\boldsymbol{\Gamma} = \begin{Bmatrix} \mathbf{M}^{-1}\mathbf{s} \\ \mathbf{0} \end{Bmatrix} = \sum_{i=1}^{n}(\eta_i\boldsymbol{\Psi}_i + \eta_i^*\boldsymbol{\Psi}_i^*) \tag{35}$$

wherein η_i and η_i^* are aforementioned modal participation coefficients. Due to the completeness of the vector bases constructed by the usual and generalized eigenvectors, the above equation always holds.

Similarly, using the time derivative of Eq. (34), introducing Eq. (17) and considering the following relation from Eq. (35), $\sum_{i=1}^{n}\boldsymbol{\rho}_i^v = \sum_{i=1}^{n}(\eta_i\boldsymbol{\chi}_i + \eta_i^*\boldsymbol{\chi}_i^*) = \mathbf{M}^{-1}\mathbf{s}$, wherein $\boldsymbol{\chi}_i$ and $\boldsymbol{\chi}_i^*$ represent the first *n* elements of $\boldsymbol{\Psi}_i$ and $\boldsymbol{\Psi}_i^*$ respectively. For under- and over-critically damped modes, $\boldsymbol{\chi}_i = \lambda_i\boldsymbol{\Phi}_i$ and $\boldsymbol{\chi}_i^* = \lambda_i\boldsymbol{\Phi}_i^*$; for critically damped modes, $\boldsymbol{\chi}_i = \lambda_i\boldsymbol{\Phi}_i$ and $\boldsymbol{\chi}_i^* = \lambda_i\boldsymbol{\Phi}_i^* + \boldsymbol{\Phi}_i$. The equivalent structural acceleration can be given by,

$$\ddot{\mathbf{u}}_a(t) = \sum_{i=1}^{n}\left[\boldsymbol{\rho}_i^a \dot{q}_i(t) + \boldsymbol{\varphi}_i^a q_i(t)\right] \tag{36}$$

wherein, $\boldsymbol{\rho}_i^a = \boldsymbol{\varphi}_i^v - 2\xi_i\omega_i\boldsymbol{\rho}_i^v$, $\boldsymbol{\varphi}_i^a = -\omega_i^2\boldsymbol{\rho}_i^v$ and $\ddot{\mathbf{u}}_a(t) = \ddot{\mathbf{u}}(t) - \mathbf{M}^{-1}\mathbf{s}f(t)$. When the excitation refers to acceleration input, $\ddot{\mathbf{u}}_a(t)$ represents the absolute acceleration response.

5. Modal truncation error estimate

In the dynamic analysis of a structure with a large number of DOFs, the usual practice is to consider only the first *m* (*m*<<*n*) modes and ignore the contribution of high vibration modes to improve the computational efficiency, namely,

$$\mathbf{y}(t) \cong \sum_{i=1}^{m}\left[\boldsymbol{\rho}_i \dot{q}_i(t) + \boldsymbol{\varphi}_i q_i(t)\right] \tag{37}$$

which can be called the complex mode displacement method (CMDM). However, the truncation error may be too large to be ignored in some cases. In this section, the source of the modal truncation error is analyzed.

The displacement and velocity responses correspond to the only *m* low modes that can be obtained respectively, utilizing Eq. (14) as,

$$\mathbf{u}_m(t) = \sum_{i=1}^{m} [\boldsymbol{\phi}_i z_i(t) + \boldsymbol{\phi}_i^* z_i^*(t)] = \boldsymbol{\Phi}_m \mathbf{z}_m(t) \tag{38}$$

$$\dot{\mathbf{u}}_m(t) = \sum_{i=1}^{m} [\boldsymbol{\chi}_i z_i(t) + \boldsymbol{\chi}_i^* z_i^*(t)] = \boldsymbol{\Phi}_m \mathbf{J}_m \mathbf{z}_m(t) \tag{39}$$

Note that $\mathbf{u}_m(t)$ and $\dot{\mathbf{u}}_m(t)$ are approximations to true responses. Therefore, the true equation of the motion of the system, i.e., Eq. (1), corresponds to $\mathbf{u}(t)$ and $\dot{\mathbf{u}}(t)$ rather than $\mathbf{u}_m(t)$ and $\dot{\mathbf{u}}_m(t)$. Another equation of motion associated with $\mathbf{u}_m(t)$ and $\dot{\mathbf{u}}_m(t)$ exists, which can be expressed as,

$$\mathbf{M}\ddot{\mathbf{u}}_m + \mathbf{C}\dot{\mathbf{u}}_m + \mathbf{K}\mathbf{u}_m = \mathbf{f}_m(t) \tag{40}$$

wherein, $\mathbf{f}_m(t)$ is the external loading corresponding to $\mathbf{u}_m(t)$ and $\dot{\mathbf{u}}_m(t)$, which differ from the actual applied loading, $\mathbf{f}(t)$.

To obtain the expression $\mathbf{f}_m(t)$, the above equation of motion is rewritten as,

$$\mathbf{A}\dot{\mathbf{v}}_m + \mathbf{B}\mathbf{v}_m = \mathbf{p}_m(t) \tag{41}$$

wherein,

$$\mathbf{v}_m = \begin{Bmatrix} \dot{\mathbf{u}}_m \\ \mathbf{u}_m \end{Bmatrix} \qquad \mathbf{p}_m(t) = \begin{Bmatrix} \tilde{\mathbf{f}}_m(t) \\ \mathbf{f}_m(t) \end{Bmatrix}$$

wherein $\tilde{\mathbf{f}}_m(t) = \mathbf{M}\boldsymbol{\Phi}_m \mathbf{a}_m^{-1} \boldsymbol{\Phi}_m^{\mathrm{T}} \mathbf{f}(t)$, which is obtained by subtracting Eq. (39) from the first-time derivative of Eq. (38). Substituting $\mathbf{v}_m(t) = \boldsymbol{\Psi}_m \mathbf{z}_m(t)$ into Eq. (41), pre-multiplying by $\boldsymbol{\Psi}_m^{\mathrm{T}}$ and recalling the first *m* pairs of equations in Eq. (6), we obtain,

$$\dot{\mathbf{z}}_m - \mathbf{J}_m \mathbf{z}_m = \mathbf{a}_m^{-1} \boldsymbol{\Psi}_m^{\mathrm{T}} \mathbf{p}_m(t) \tag{42}$$

For the purpose of comparison, the first *m* pairs of equation of motion in Eq. (15) are written again as follows,

$$\dot{\mathbf{z}}_m(t) - \mathbf{J}_m\, \mathbf{z}_m(t) = \mathbf{a}_m^{-1} \boldsymbol{\Phi}_m^{\mathrm{T}} \mathbf{f}(t) \tag{43}$$

The comparison between Eq. (42) and Eq. (43), according to the first *m* sets of eigenvalue equations in Eq. (6), yields,

$$\begin{aligned} \mathbf{p}_m(t) &= (\boldsymbol{\Psi}_m^{\mathrm{T}})^{-1} \boldsymbol{\Phi}_m^{\mathrm{T}} \mathbf{f}(t) = \mathbf{A}\boldsymbol{\Psi}_m \mathbf{a}_m^{-1} \boldsymbol{\Phi}_m^{\mathrm{T}} \mathbf{f}(t) \\ &= \begin{bmatrix} \mathbf{M}\boldsymbol{\Phi}_m \mathbf{a}_m^{-1} \boldsymbol{\Phi}_m^{\mathrm{T}} \\ -\mathbf{K}\boldsymbol{\Phi}_m \mathbf{J}_m^{-1} \mathbf{a}_m^{-1} \boldsymbol{\Phi}_m^{\mathrm{T}} \end{bmatrix} \mathbf{f}(t) \end{aligned} \tag{44}$$

$\mathbf{f}_m(t)$ can then be given by,

$$\mathbf{f}_m(t) = \mathbf{s}_m f(t) \tag{45}$$

wherein $\mathbf{s}_m = -\mathbf{K}\boldsymbol{\Phi}_m \mathbf{J}_m^{-1} \mathbf{a}_m^{-1} \boldsymbol{\Phi}_m^{\mathrm{T}} \mathbf{s}$.

Considering the orthogonality conditions in Section 3.2, it can be observed that $\mathbf{p}_m(t)$ is orthogonal to the truncated vibration modes. In other words, the inaccuracies in the truncated mode superposition analysis are caused by load components that are normal to the modes included in the analysis, and the force error vector can be expressed as,

$$\mathbf{e}_m = \mathbf{f}(t) - \mathbf{f}_m(t) = [\mathbf{I} + \mathbf{K}\boldsymbol{\Phi}_m \mathbf{J}_m^{-1} \mathbf{a}_m^{-1} \boldsymbol{\Phi}_m^{\mathrm{T}}] \mathbf{f}(t) \tag{46}$$

wherein $\mathbf{I}$ represents an identity matrix of order *n*. A more practical form of the modal truncation error can be expressed in terms of the Euclidean norm ($|\mathbf{x}|_2 = \sqrt{\mathbf{x}^{\mathrm{T}}\mathbf{x}}$),

$$e_m = \frac{|\mathbf{f}(t) - \mathbf{f}_m(t)|_2}{|\mathbf{f}(t)|_2} = \frac{|\mathbf{s} - \boldsymbol{s}_m|_2}{|\mathbf{s}|_2} \tag{47}$$

According to Eqs. (A2) and (A4) in the Appendix A, e_m ranges from 0, denoting no modes used, to 1, if all modes are included in the analysis. Therefore, it can be used as an indicator to evaluate the modal truncation error. In the case of large errors, corrected methods are proposed in the following section to improve the results.

6. Corrected methods for modal truncation

6.1 Corrections for structural displacement

It is widely known that the response of higher frequency modes can be calculated using static analysis, since their inertial effects are negligible (Clough and Penzien 1995), i.e., ignoring the acceleration and velocity terms on the left hand side of Eq. (17). In order to take advantage of this fact, the mode displacement superposition equation presented by Eq. (33) needs to be divided into two parts: the sum of the lower mode contribution and the sum of the remaining higher modes for which the dynamic amplification effects may be neglected. Thus, Eq. (33) becomes,

$$\begin{aligned} \mathbf{u}(t) &= \sum_{i=1}^{m} \left[\boldsymbol{\rho}_i^d \dot{q}_i(t) + \boldsymbol{\varphi}_i^d q_i(t) \right] \\ &\quad + \sum_{i=m+1}^{n} \left[\boldsymbol{\rho}_i^d \dot{q}_i(t) + \boldsymbol{\varphi}_i^d q_i(t) \right] \\ &\cong \mathbf{u}_d(t) + \mathbf{u}_s(t) \end{aligned} \tag{48}$$

wherein the subscript *d* identifies the response from the modes that are subjected to dynamic amplification effects, while the subscript *s* denotes the response that can be approximated by static analysis.

The responses $\dot{q}_i(t)$ and $q_i(t)$ given by each of the first *m* modes may be calculated by any standard SDOF dynamic analysis procedure. For each of the ordinary remaining *n–m* modes, the response $\dot{q}_i(t)$ can be ignored due to the negligible inertial effect, and $q_i(t)$ at any time *t* may be obtained using ordinary static analysis. Recalling the discussions in Section 5, the approximated structural response of the first *m* modes, corresponding to the applied loading $\mathbf{f}_m(t)$, can be improved by adding the static response to the truncated loading $\mathbf{f}(t) - \mathbf{f}_m(t)$. Using Eq. (46), the static contribution of the remaining *n–m* modes to the displacement can be given by,

$$\begin{aligned} \mathbf{u}_s(t) &= \mathbf{K}^{-1}[\mathbf{f}(t) - \mathbf{f}_m(t)] \\ &= (\mathbf{K}^{-1} + \boldsymbol{\Phi}_m \mathbf{J}_m^{-1} \mathbf{a}_m^{-1} \boldsymbol{\Phi}_m^{\mathrm{T}}) \mathbf{f}(t) \\ &= \left(\mathbf{K}^{-1}\mathbf{s} - \sum_{i=1}^{m} \frac{\boldsymbol{\varphi}_i^d}{\omega_i^2} \right) f(t) \end{aligned} \tag{49}$$

Note that the static responses associated with higher modes is calculated using only the obtained lower modes, and the evaluation of the higher mode shapes is avoided in order to reduce large computations.

The total response equation, including this static correction, is obtained by substituting Eq. (49) into Eq. (48) with the following final result,

$$\mathbf{u}(t) \cong \sum_{i=1}^{m}\left[\boldsymbol{\rho}_i^d \dot{q}_i(t) + \boldsymbol{\varphi}_i^d q_i(t)\right] + \left(\mathbf{K}^{-1}\mathbf{s} - \sum_{i=1}^{m}\frac{\boldsymbol{\varphi}_i^d}{\omega_i^2}\right) f(t) \tag{50}$$

wherein the first term represents complex mode displacement superposition analysis using m modes and the other term is the corresponding static correction for the higher (n–m) modes. A computer solution using this formulation only requires the addition of the correction term, which is given as the product of a constant vector and the loading amplitude factor $f(t)$, to the standard mode displacement solution for m modes.

Following the derivation procedure of the conventional mode acceleration method (MAM) (Clough and Penzien 1995), the complex mode acceleration method (CMAM), which is an equivalent form of Eq. (50), can be expressed as

$$\mathbf{u}(t) \cong \mathbf{K}^{-1}\mathbf{s}f(t) + \sum_{i=1}^{m}\left[\left(\boldsymbol{\rho}_i^d - \frac{2\xi_i}{\omega_i}\boldsymbol{\varphi}_i^d\right)\dot{q}_i(t) - \frac{1}{\omega_i^2}\boldsymbol{\varphi}_i^d \ddot{q}_i(t)\right] \tag{51}$$

In this method, the response is represented by static contribution as well as the dynamic amplification effect of the applied loading having a negligible influence in response to the higher modes.

Apparently, the methods proposed previously are the development of the conventional mode superposition method. When the damping matrix becomes classical and the complex modes are normalized by the same rule as undamped modes, the proposed methods can be automatically reduced to the conventional method (see Appendix B for more details).

6.2 Correction for structural acceleration

In practice, a system typically consists of a primary structure and some secondary structures. Often, we are not concerned only with the response of the primary structure for life safety but also with secondary structures for economic costs such as the damage of non-structural components or equipment due to rocking, falling or slip motions in an earthquake. Acceleration response refers to an interested quantity for the design of secondary structures (Lu *et al*. 2014, Lu *et al*. 2016, Chen *et al*. 2014, Pozzi1 and Der Kiureghian 2015). To reduce the computation scale for large practical structures, modal truncation is always required in an acceleration analysis using Eq. (36). The correction concept can be introduced into the process of acceleration calculations to improve the final result.

According to the procedure of the static correction method, neglecting the dynamic contributions of the higher modes and considering Eq. (35), the improved mode superposition method for the structural acceleration can be expressed as,

$$\ddot{\mathbf{u}}_a(t) \cong \sum_{i=1}^{m}\left[\boldsymbol{\rho}_i^a \dot{q}_i(t) + \boldsymbol{\varphi}_i^a q_i(t)\right] - \left[\mathbf{M}^{-1}\mathbf{s} + \sum_{i=1}^{m}\frac{\boldsymbol{\varphi}_i^a}{\omega_i^2}\right] f(t) \tag{52}$$

wherein, the second term on the right side continues to be the static contribution from higher modes. Only the lower modes are required to evaluate the acceleration response. Eqs. (50)-(52) have similar expressions and can be used conveniently in practice. In this paper, both are uniformly called CMAM due to the common assumption.

7. Application examples

7.1 Example 1

This example is taken from the paper of Liu *et al*. (2005), which is a planar ten-story shear-type structure with constant mass and stiffness coefficients for each story: m=2.5×10^5(kg), k=4.5×10^5 (kN/m). The inherent structure damping ratios for all modes are assumed as $\xi_i = 0.03$. Fifty linear viscous dampers with damping coefficients of 3.5×10^6(Ns/m) are installed in this building to reduce the earthquake-induced response, and the optimized device configuration (see the paper of Liu *et al*. (2005) for more details regarding the optimization) is illustrated in Fig. 1.

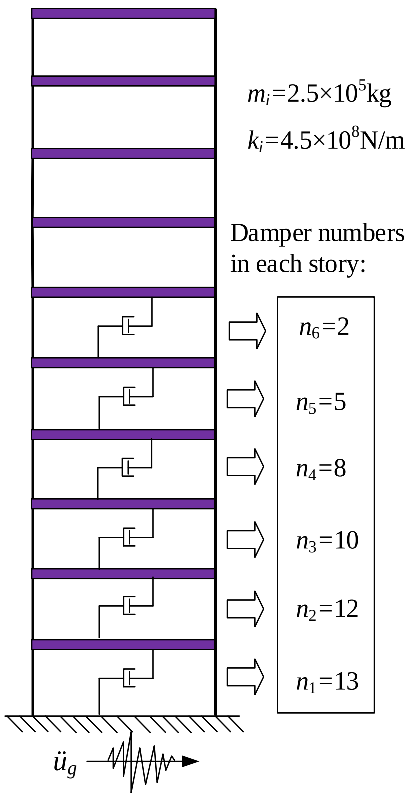

Fig. 1 Analysis model and structural parameters

Table 1 Natural frequencies (ω) and modal damping ratios (ξ)

Mode	1	2	3	4	5	6	7	8	9	10
ω(rad/s)	6.53	21.14	41.05	47.34	49.19	54.39	64.68	67.87	74.59	80.47
ξ	0.23	0.27	0.34	0.96	0.20	1.79	2.67	0.07	3.63	0.038

Table 1 depicts the natural frequencies and modal damping ratios of the structure with supplemental energy dissipation devices. The first modal damping ratio can be observed to be 0.23, which is in the range close to 0.20, as suggested by Occhiuzzi (2009), and indicates that this structure is a regular seismic protection system with an appropriate added damping level. The forth modal damping ratio is close to the critical damping, and the sixth, seventh and ninth ratios exceed 1.0. This example also demonstrates that the problem of over-critical damping may be very common, since we always pay more attention to the lower modes in practical designs.

The ground motions used in the study are obtained using the simulation method suggested by Ruiz and Penzien (1968). In this method, the ground acceleration records are generated as samples of a filtered white-noise process modulated by an intensity function. The intensity function used here is defined by Amin and Ang (1968) and includes a stationary strong-motion phase of 10s (between 10 and 20s). The filtered Kanai-Tajimi model suggested by Ruiz and Penzien (1969) was selected as the power spectral density (PSD) of the filtered white-noise process,

$$S_{\ddot{u}_g}(\omega) = S_0 \frac{\omega_g^4 + 4\xi_g^2\omega_g^2\omega^2}{\left(\omega_g^2-\omega^2\right)^2 + 4\xi_g^2\omega_g^2\omega^2} \frac{\omega^4}{\left(\omega_f^2-\omega^2\right)^2 + 4\xi_f^2\omega_f^2\omega^2} \tag{53}$$

wherein S_0 is a scale factor, ω_g and ξ_g are the filter parameters representing natural frequency and the damping ratio of the soil layer respectively. ω_f and ξ_f denote the parameters of a secondary filter that are introduced to ensure finite variance of the ground displacement. By specifying the different parameters for Eq. (53), the input can be regarded as a wide- or narrow-band excitation. For instance, if we consider a firm soil site with the following parameters $\omega_g = 15\text{rad/s}$, $\omega_f = 1.5\text{rad/s}$, $\xi_g = 0.6$ and $\xi_f = 0.6$, this input can be considered as a wide-band input (see Fig. 2). However, if we consider a soft soil site with $\omega_g = 5\text{rad/s}$, $\omega_f = 0.5\text{rad/s}$, $\xi_g = 0.2$ and $\xi_f = 0.6$, this input can be more reasonably regarded as a narrow-band excitation. The scale factor S_0 is selected such that a mean peak ground acceleration of 0.4g is reached when the duration of the record is 30s.

Fig. 3 depicts the frequency response functions of the first story under base acceleration excitations, which are obtained by assuming $f(t)$ in Eq. (1) as $e^{i\omega t}$ and using Eqs. (33) and (36). The amplitudes are normalized by the exact maximum amplitude. The black solid line indicates the function evaluated from the complex and real (over-critically) damped modes, and the red dotted line depicts the function evaluated from the complex modes alone. It can be observed that the over-critically damped modes mainly impact the displacement within the lower input frequency range. In comparison with the displacement, the impact of the over-critically damped modes on the absolute acceleration is very significant within the whole range of input frequencies. Therefore, it can be predicted that the contribution of the over-critically damped modes to the displacement is important for seismic excitations from the

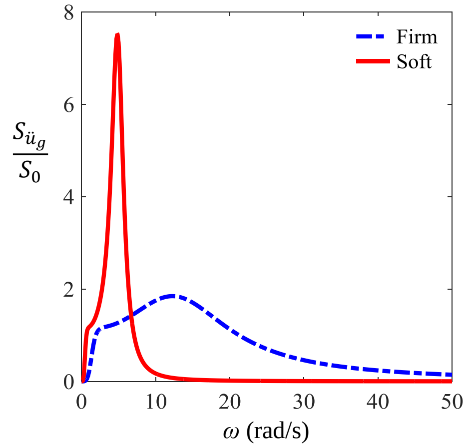

Fig. 2 Power spectral density shapes for filtered white-noise input

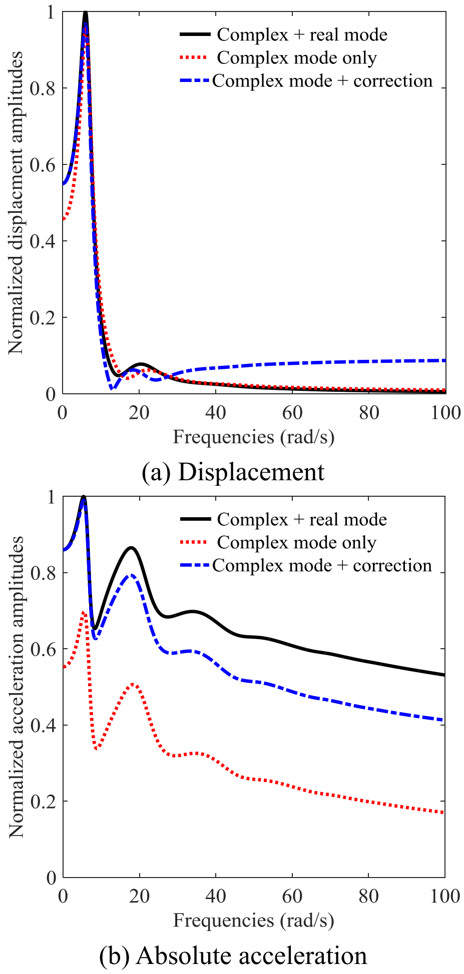

Fig. 3 Amplitudes of the frequency response function of the first

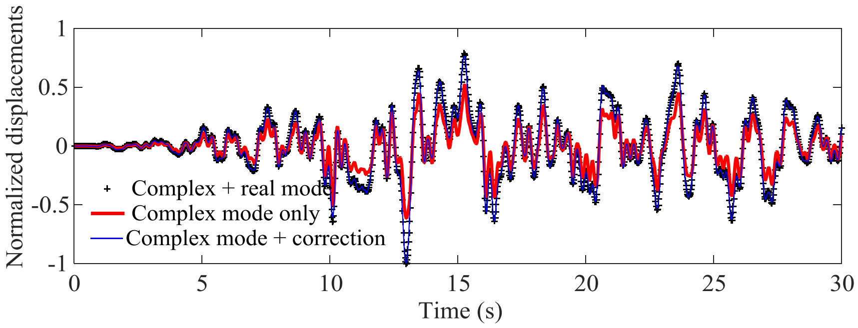

(a) Displacement time-history

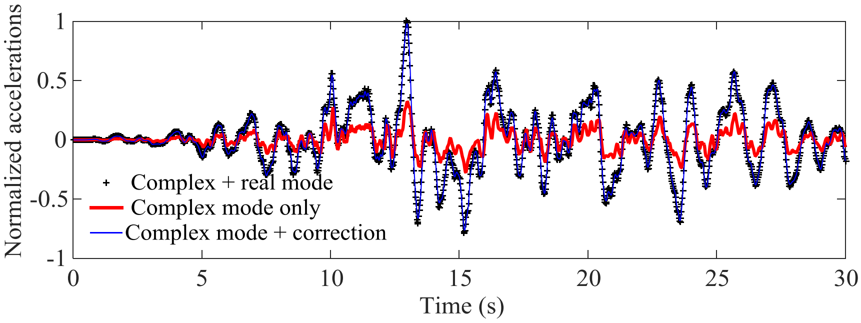

(b) Absolute acceleration time-history

Fig. 4 Dynamic responses of the first story to a sample of simulated excitations from the soft soil site

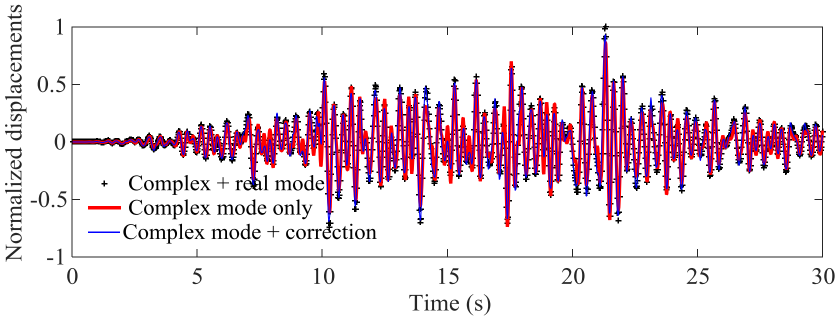

(a) Displacement time-history

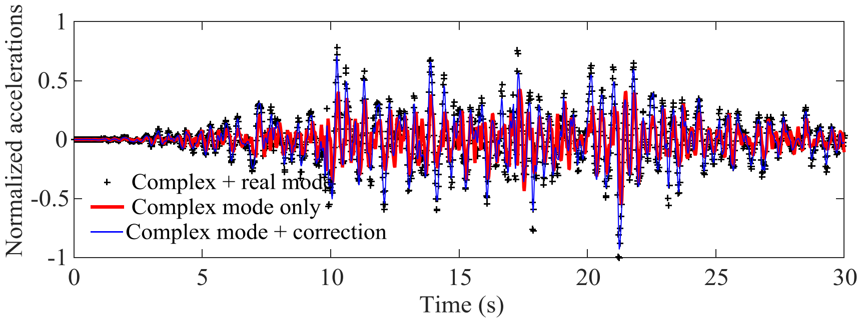

(b) Absolute acceleration time-history

Fig. 5 Dynamic responses of the first story to a sample of simulated excitations from the firm soil site

soft soil site only. For seismic excitations from soft or firm soil sites, the impact of the over-critically damped modes on the absolute acceleration is never neglectable.

The conclusion above can be verified via a time-history analysis based on the mode superposition method (Eqs. (33) and (36)). Two samples of the simulated excitations are used in the dynamic analysis—one from the soft soil site and the other from the firm soil site. Figs. 4-5 depict the time-history responses of the first story to the two base accelerations, and the responses are normalized by corresponding the maximum response estimates from the numerical integration method. From Fig. 4, it can be observed that the over-critically damped modes have significant effects on the displacement and the absolute acceleration to the excitation of the soft soil site. However, for the excitation of the firm soil site, the over-critically damped modes have an ignorable impact on the displacement, while the effect on the absolute acceleration is still significant, as shown in Fig. 5.

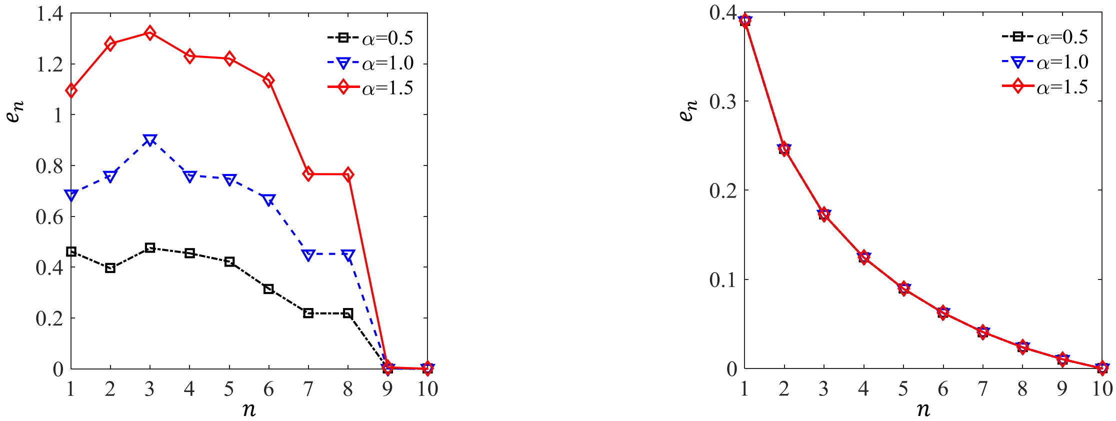

(a) Optimized damper configuration (b) Uniform damper configuration

Fig. 6 Modal truncation errors for the applied loading

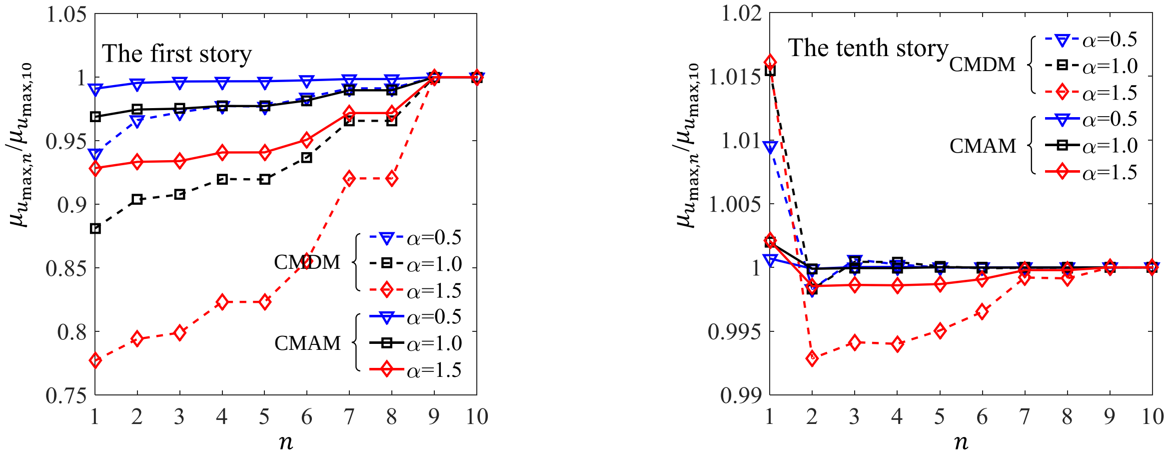

(a) Displacement

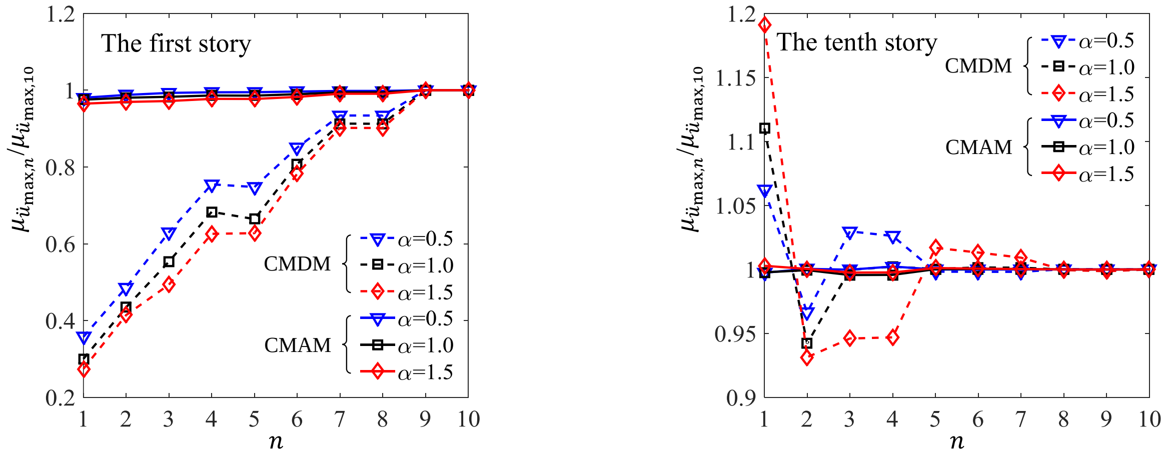

(b) Absolute acceleration

Fig. 7 Comparisons between CMAM and CMDM under excitations from the soft soil site

Figs. 3-4 also show the responses of the over-critically damped modes approximated by the corresponding static responses. Apparently, the responses with the correction can be improved significantly. Therefore, this scheme can be viewed as an alternative to consider the contribution of over-critically damped modes.

The impact of the added damping on the dynamic properties of the structure is significant. In this study, assume that each damper has a damping coefficient of $\alpha\times3.5\times10^6$(Ns/m), where the modified factor α is selected as 0.5, 1.0 and 1.5, and the damper configuration retains the same. Fig. 6 demonstrates the modal truncation errors for applied loading with respect to the number of included modes. For the sake of comparison, the modal truncation errors for the uniform damper configuration is also provided, wherein the structure is a classical damping system. It is very evident that a large difference exists between the classically and non-classically damped

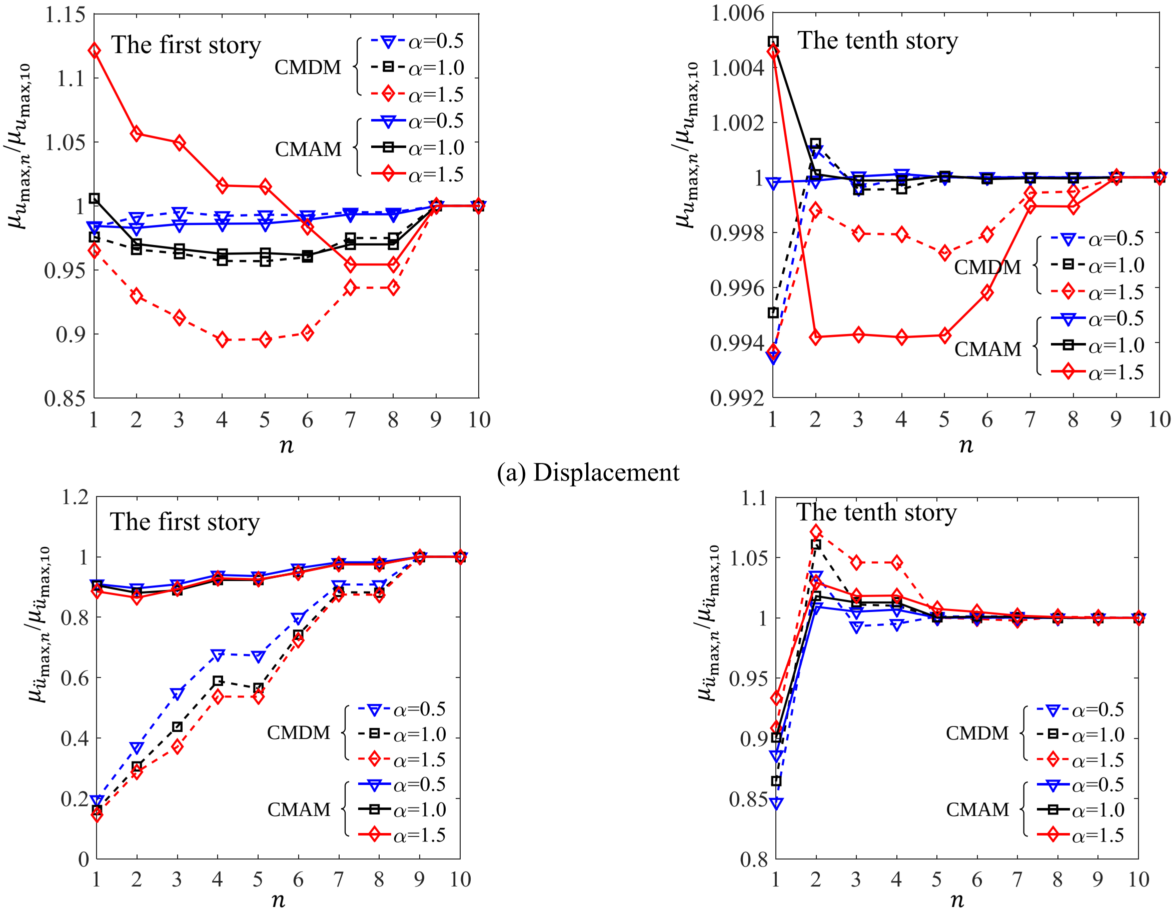

(a) Displacement

(b) Absolute acceleration

Fig. 8 Comparisons between CMAM and CMDM under excitations from the firm soil site

systems. For the optimized damper configuration (the non-classically damped system), the level of the added damping plays a significant role in the contribution of each mode to the applied loading, and the convergence rate of the error is exponentially slower than that of the classically damped system.

To examine the accuracy of the proposed method in this paper, Figs. 7-8 depict the comparisons of structural responses using CMAM and CMDM. Two groups of simulated ground motions are used in the dynamic analysis. Each group consists of 100 samples: one group comes from the soft soil site while the other corresponds to the firm soil site. In each figure, each curve represents the mean value of the maximum responses to 100 excitations as a function of the number of modes included in the analysis. Three curves with a solid line denote CMAM, and the other three with a dotted line denote CMDM. Moreover, the square, diamond and triangular symbols in these curves are used to represent different added damping levels. Since the ground motions of the soft soil site are narrow-band excitations and their dominant frequencies are lower than the fundamental natural frequency, the static correction of CMAM is very effective, as depicted in Fig. 7, especially for the absolute acceleration where only one mode can reach higher accuracy in the CMAM. It can also be observed that increasing the added damping level improves the effectiveness of the CMAM due to an increase in the first three natural frequencies. However, as seen in Fig. 8(a), the effectiveness of CMAM for the first-story drift to the excitations of the firm soil site is not well due to the wider band of the inputs. Differing from the displacement, the effectiveness of CMAM for the first-story absolute acceleration in Fig. 8(b) gets insignificantly influenced by the input frequency content.

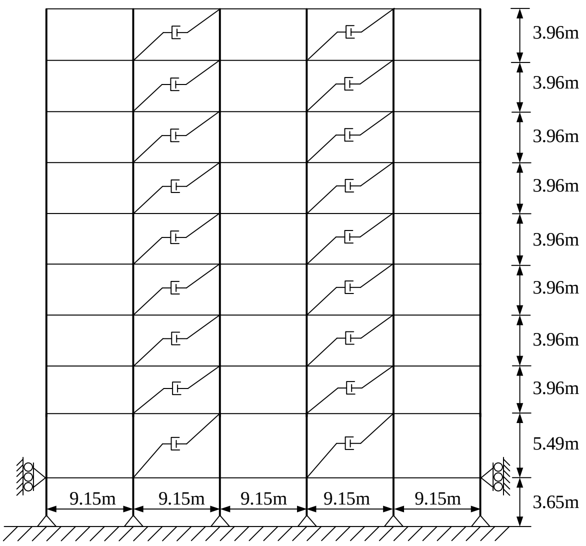

Fig. 9 The benchmark model and damper configuration

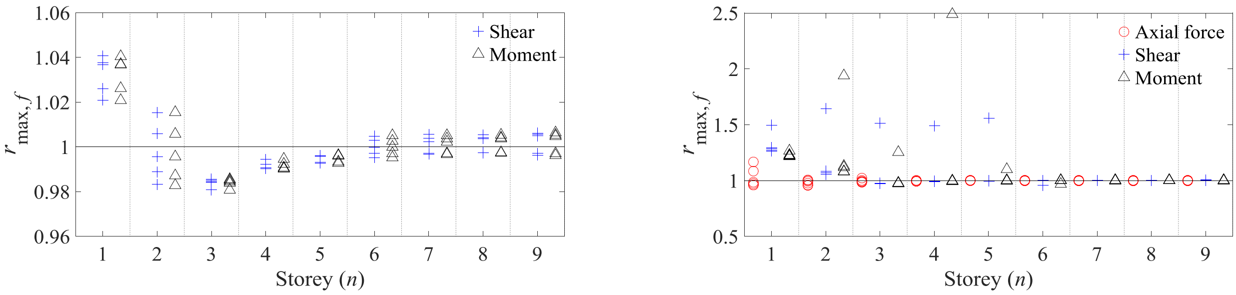

(a) Beam (b) Column

Fig. 10 Effect of the over-critically damped mode on the internal force in each frame member

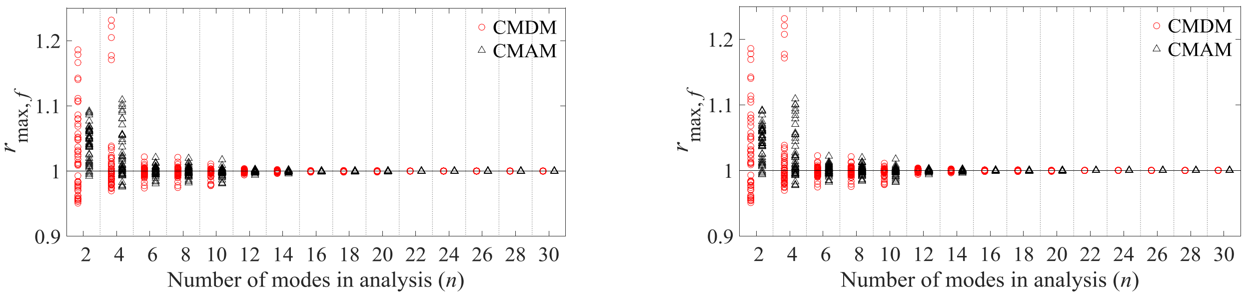

(a) Beam shear (b) Beam moment

Fig. 11 Effect of the number of modes included in analysis on the beam internal force

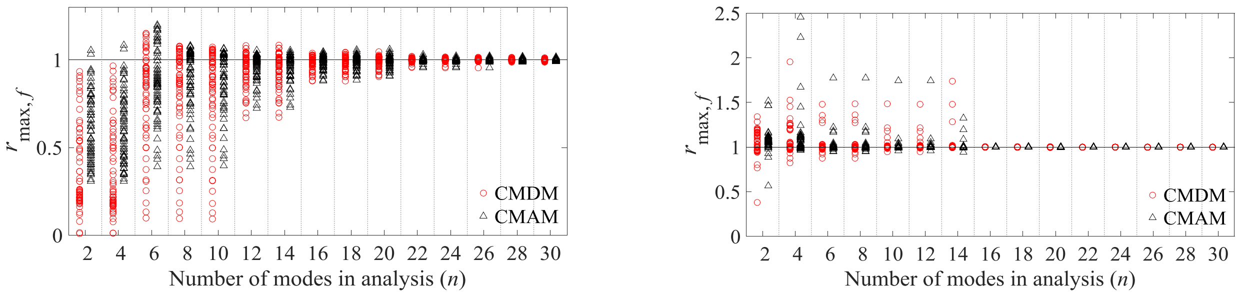

(a) Column axial force (b) Column shear

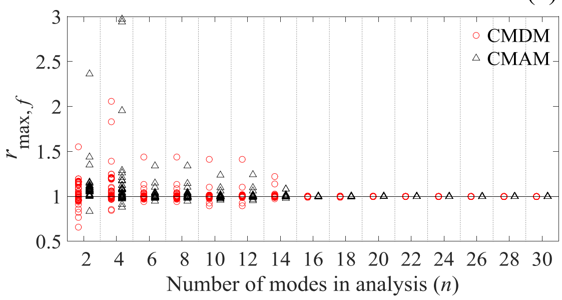

(c) Column moment

Fig. 12 Effect of the number of modes included in analysis on the column internal force

7.2 Example 2

This example is a nine-storey benchmark steel structure (Ohtori *et al.*, 2004). Viscous dampers are arranged in the structure as shown in Fig. 9. The damping coefficients of the dampers arranged in the first storey are 18×10^6N/(m/s), those in the second and third stories are 6×10^6N/(m/s) and the others are 3×10^6N/(m/s). Considering the contribution of these dampers, the first ten natural frequencies are 2.83 rad/s, 7.83 rad/s, 14.46 rad/s, 22.22 rad/s, 26.84 rad/s, 29.78 rad/s, 30.61 rad/s, 31.80 rad/s, 32.55 rad/s and 37.42 rad/s, and the first ten modal damping ratios are 0.13, 0.31, 0.40, 0.44, 1.24, 0.02, 0.03, 0.17, 0.45 and 0.16. Evidently, the fifth mode is over-critically damped. The effect of this mode on the structural response is investigated in this example by using the proposed complex mode superposition method. The seismic excitations are the N-S and U-P (vertical) components of El Centro acceleration records with the peak accelerations of 0.35g and 0.21g.

Fig. 10 illustrates the ratio of maximum internal force without the over-critically damped mode (the fifth mode) to that with this mode. Each point in the figure represents an individual member. Note that the ratio can be less and larger than one. The value of $r_{\max,f} < 1$ implies that the internal force induced by the over-critically damped mode has the same direction as that of the total force, while $r_{\max,f} > 1$ is reverse. It can be seen that the effect of the over-critically damped mode is very significant, particularly for the first five storeys, e.g., the beam force can increase by 4% or decrease by 2% and the maximum column shear and moment in the fourth storey are respectively enlarged to 1.5 and 2.5 times. Figs. 11-12 show the maximum internal forces of all beams and columns as a function of the number of modes included in the analysis, normalized by the exact responses computed using all mode vectors. It is clearly observed that the CMAM has a better accuracy than that of CMDM because of the contribution of the static correction in CMAM with the same number of complex modes used.

8. Summary and conclusions

To conduct a dynamic analysis of heavily damped systems, a generalized complex mode superposition method that is suitable for systems with under-critical, critical and over-critical modal damping is proposed and expressed in a unified form for structural displacement, velocity and acceleration responses. In this method, the conventional algorithms of eigenvalue problems continue to be valid, even though the system becomes defective due to critical modal damping. The application of this method is convenient in practice and not restricted by the damping level. Based on the modal truncation error analysis, corrected methods for displacement and acceleration responses are developed to consider the contribution of the truncated higher modes. These methods are very practical for decreasing computations, particularly with respect to large engineering structures. The method proposed in the present paper is a development of the conventional complex mode superposition method. When complex modes are normalized by the same rule as undamped modes, the proposed methods can automatically degenerate to conventional methods. The numerical examples show that the issue of over-critically damped modes always exists in the commonly used passive control structures and the over-critically damped modes play an important role in structural responses. The numerical results also show that the effectiveness of the CMAM proposed in this paper is significant, particularly for the acceleration response and internal forces of frame members. Through the studies discussed in this paper, the application range of dynamic analyses based on the mode superposition method can be expanded significantly.

Acknowledgement

This work was supported by the National Natural Science Foundation of China (Grant no. 51808154), the National Key R&D Program of China (Grant no.2017YFC0703600) and the Scientific Research Founding for introduced talents of Guangzhou University (Grant no.2809952).

References

Akgu, M.A. (1993), "A new family of mode-superposition methods for response calculations", *J Sound Vib.*, **167**(2), 289-302. https://doi.org/10.1006/jsvi.1993.1336.

Amin, M. and Ang, A. (1968), "Nonstationary stochastic model of earthquake motions", *J Eng Mech ASCE*, **94**(2), 559-583.

Benfratello, S. and Muscolino, G. (2001), "Mode-superposition correction method for deterministic and stochastic analysis of structural systems", *Comput Struct.*, **79**(26-28), 2471-2480. https://doi.org/10.1016/S0045-7949(01)00084-0.

Besselink, B., Tabak, U., Lutowska, A., Wouw, N., Nijmeijer, H., Rixen, D.J., Hochstenbach, M.E. and Schilders, W.H.A. (2013), "A comparison of model reduction techniques from structural dynamics, numerical mathematics and systems and control", *J Sound Vib.*, **332**(19), 4403-4422. https://doi.org/10.1016/j.jsv.2013.03.025.

Cacciola, P., Maugeri, N. and Muscolino, G. (2007), "A modal correction method for non-stationary random vibrations of linear systems", *Probab. Eng. Mech.*, **22**(2), 170-180. https://doi.org/10.1016/j.probengmech.2006.10.002.

Camarda, C.J., Haftka, R.T. and Riley, M.F. (1987), "An evaluation of higher-order modal methods for calculating transient structural response", *Comput Struct.*, **27**(1), 89-101. https://doi.org/10.1016/00457949(87)90184-2.

Chen, H.T., Tan, P. and Zhou, F.L. (2017a), "An improved response spectrum method for non-classically damped systems", *Bull. Earthq. Eng.*, **15**(10), 4375-4397. https://doi.org/10.1007/s10518-017-0144-4.

Chen, H.T., Tan, P., Ma, H.T. and Zhou, F.L. (2017b), "Response spectrum analysis considering non-classical damping in the base-isolated benchmark building", *Struct. Eng. Mech.*, **64**(4), 473-485. https://doi.org/10.12989/sem.2017.64.4.473.

Chen, J., Xu, R. and Zhang, M. (2014), "Acceleration response spectrum for predicting floor vibration due to occupant walking", *J Sound Vib.* **333**(15), 3564-3579. https://doi.org/10.1016/j.jsv.2014.03.023.

Chu, Y.L., Song, J.W. and Lee, G.C. (2009), "Modal analysis of arbitrarily damped three-dimensional linear structures subjected to seismic excitations", *Technical Report*, MCEER-09-0001, University of Buffalo, State University of New York.

Clough, R. and Penzien, J. (1995), *Dynamics of Structures*, (3rd Edition), Computers and Structures Inc., California.

Cornwell, R.E., Craig, R.R. and Johnston, C.P. (1983), "On the application of the mode acceleration method to structural dynamics problems", *Earthq Eng Struct Dyn.*, **11**(5), 679-688. https://doi.org/10.1002/eqe.4290110507.

Der Kiureghian, A. and Nakamura, Y. (1993), "CQC modal combination rule for high-frequency modes", *Earthq Eng Struct Dyn.*, **22**(11), 943-956. https://doi.org/10.1002/eqe.4290221103.

Dhileep, M. and Bose, P.R. (2008), "A comparative study of "missing mass" correction methods for response spectrum method of seismic analysis", *Comput Struct.*, **86**(21-22), 2087-2094. https://doi.org/10.1016/j.compstruc.2008.04.003.

Dickens, J.M., Nakagawa, J.M. and Wittbrodt, M.J. (1997), "A critique of mode acceleration and modal truncation augmentation methods for modal response analysis", *Comput Struct.*, **62**(6), 985-998. https://doi.org/10.1016/s0045-7949(96)00315-x.

Dickens, J.M. and Pool, K.V. (1992), "Modal truncation vectors and periodic time domain analysis applied to a cyclic symmetry structure", *Comput Struct.*, **45**(4), 685-696. https://doi.org/10.1016/0045-7949(92)90487-k.

FEMA 273 (1997), *NEHRP guidelines for the seismic rehabilitation of buildings*. The Federal Emergency Management

Agency; Washington, USA.

Friswell, M., Prells, U. and Garvey, S. (2005), "Low-rank damping modifications and defective systems", *J Sound Vib.*, **279**(3-5), 757-774. https://doi.org/10.1016/j.jsv.2003.11.042.

Hansteen, O.E. and Bell K. (1979), "On the accuracy of mode superposition analysis in structural dynamics", *Earthq Eng Struct Dyn*. **7**(5), 405-411. https://doi.org/10.1002/eqe.4290070502.

Huang, C., Liu, Z.S. and Chen, S.H. (1997), "An accurate modal method for computing response to periodic excitation", *Comput Struct.*, **63**(3), 625-631. https://doi.org/10.1016/s0045-7949(96)00367-7.

Liu, G.H., Lian, J.J. and Liang, C. (2016) "Completeness verification of complex response spectrum method for underdamped and overdamped systems regarding the decoupled damping as mathematical parameter without physical meaning", *J. Earthq. Eng.*, **20**(7), 1104-1125. https://doi.org/10.1080/13632469.2016.113 8165.

Li, L., Hu, Y. and Wang, X. (2013), "Improved approximate methods for calculating frequency response function matrix and response of MDOF systems with viscoelastic hereditary terms", *J Sound Vib.*, **332**(15), 3945-3956. https://doi.org/10.1016/j.jsv.2013.01.043.

Li, L., Hu, Y., Wang, X. and Lü, L. (2014), "A hybrid expansion method for frequency response functions of non-proportionally damped systems", *Mech Syst Signal Pr.*, **42**(1-2), 31-41. https://doi.org/10.1016/j.ymssp.2013.07.020.

Liu, W., Tong, M. and Lee, G.C. (2005), "Optimization methodology for damper configuration based on building performance indices", *J. Struct. Eng.*, **131**(11), 1746-1756. https://doi.org/10.1061/(ASCE)0733-9445(2005)131:11(1746).

Liu, Z.S., Wang, K., Huang, C. and Chen, S.H. (1996), "An extended hybrid method for contribution due to truncate lower- and higher-frequency modes in modal summation", *Eng Struct.*, **18**(7), 558-563. https://doi.org/10.1016/0141-0296(95)00123-9.

Lu, L., Chen, P. and Pong, K. (2016), "Theory and experiment of an inertia-type vertical isolation system for seismic protection of equipment", *J Sound Vib.*, **366**(31), 44-61. https://doi.org/10.1016/j.jsv.2015.12.009.

Lu, L.Y., Hung, J.H. and Lin, P.Y. (2014), "Seismic simulation test of equipment protection by using a fuzzy-controlled smart isolation system", *J Vib Control.*, **20**(16), 2501-2520. https://doi.org/10.1177/1077546313479989.

Maddox, N.R. (1975), "On the number of modes necessary for accurate response and resulting forces in dynamic analyses", *J Appl Mech ASME*, **42**(2), 516-517. https://doi.org/10.1115/1.3423622.

Mentrasti, L. (2012), "Exact deflation in the complex modal analysis of low-rank non-classically damped structures", *Eng. Struct.*, **45**, 496-508. https://doi.org/10.1016/j.engstruct.2012.06.023.

Moler, C.B. and Stewart, G.W. (1973), "An algorithm for generalized matrix eigenvalue problems", *SIAM J. Num. Anal.*, **10**(2), 241-256. https://doi.org/10.1137/0710024.

Occhiuzzi, A. (2009), "Additional viscous dampers for civil structures: analysis of design methods based on effective evaluation of modal damping ratios", *Eng. Struct.*, **31**(5), 1093-1101. https://doi.org/10.1016/j.engstruct.2009.01.006

Ohtori, Y., Christenson, R.E., Spencer Jr., B.F. and Dyke, S.J. (2004) "Benchmark control problems for seismically excited nonlinear buildings", *J. Eng. Mech.*, **130**(4), 366-385. https://doi.org/10.1061/(ASCE)0733-9399(2004)130:4(366).

Pozzi1, M. and Der Kiureghian, A. (2015), "Response spectrum analysis for floor acceleration", *Earthq Eng Struct. Dyn.*, **44**(12), 2111-2127. https://doi.org/10.1002/eqe.2583.

Qu, Z.-Q. (2000), "Hybrid expansion method for frequency responses and their sensitivities, Part I: Undamped systems", *J Sound Vib.*, **231**(1), 175-193. https://doi.org/10.1006/jsvi.1999.2672.

Qu, Z.-Q. and Selvam, R.P. (2000), "Hybrid expansion method for frequency responses and their sensitivities, Part II: Viscously damped systems", *J Sound Vib.*, **238**(3), 369-388. https://doi.org/10.1006/jsvi.2000.3085.

Ruiz, P. and Penzien, J. (1968), "PSEAGN-artificial generation of earthquake accelerograms", *Report of Earthquake Engineering Research Center*, No. UCB/EERC69-3, University of California, Berkeley, California.

Ruiz, P. and Penzien, J. (1969), Probabilistic study of behavior of structures during earthquakes. *Report of Earthquake Engineering Research Center*, No. EERC 69-3, University of California, Berkeley, California.

Singh, M.P. (1980), "Seismic response by SRSS for non-proportional damping", *J. Eng. Mech. ASCE*, **106**(6), 1405-1419. https://doi.org/10.1243/03093247V154235.

Singh, M.P. and McCown, B.E. (1986), "Mode acceleration-based response spectrum approach for non-classically damped structures", *Soil Dyn Earthq Eng.*, **5**(4), 226-233. https://doi.org/10.1016/0267-7261(86)90008-4.

Sivandi-Pour, A., Gerami, M. and Khodayarnezhad, D. (2014), "Equivalent modal damping ratios for non-classically damped hybrid steel concrete buildings with transitional storey", *Struct. Eng. Mech.*, **50**(3), 383-401. https://doi.org/10.12989/sem.2014.50.3.383.

Suarez, L.E. and Gaviria, C.A. (2015), "Dynamic properties of a building with viscous dampers in non-proportional arrangement", *Struct. Eng. Mech.*, **55**(6), 1241-1260. https://doi.org/10.12989/sem.2015.55.6.1241.

Takewaki, I. (2004), "Frequency domain modal analysis of earthquake input energy to highly damped passive control structures", *Earthq Eng Struct Dyn.*, **33**(5), 575-590. https://doi.org/10.1002/eqe.361.

Traill-Nash, R.W. (1981), "Modal methods in the dynamics of systems with non-classical damping", *Earthq Eng Struct Dyn.*, **9**(2), 153-169. https://doi.org/10.1002/eqe.4290090205.

Uriz, P. and Whittaker, A. (2001), "Retrofit of pre-Northridge steel moment-resisting frames using fluid viscous dampers", *Struct. Design Tall Build.*, **10**(3), 71-90. https://doi.org/10.1002/tal.199.

Veletsos, A.S. and Ventura, C.E. (1986), "Modal analysis of non-classically damped linear systems", *Earthq. Eng. Struct. Dyn.*, **14**(2), 217-243. https://doi.org/10.1002/eqe.4290140205.

Whittle, J., Williams, M., Karavasilis, T. and Blakeborough, A. (2012), "A comparison of viscous damper placement methods for improving seismic building design", *J. Earthq. Eng.*, **16**(4), 540-560. https://doi.org/10.1080/13632469.2011.653864.

Xiao, W.W., Li, L. and Lei, S. (2017), "Accurate modal superposition method for harmonic frequency response sensitivity of non-classically damped systems with lower-higher-modal truncation", *Mech. Syst. Signal Pr.*, **85**, 204-217. http://dx.doi.org/10.1016/j.ymssp.2016.08.017.

Yu, R.F., Wang, L., Liu, H. and Zhou, X.Y. (2005), "The CCQC3 Method for Multi-component Seismic Response of Non-classically Damped Irregular Structures", *Structures Congress*, New York, April.

Yu, R.F. and Zhou, X.Y. (2008), "Response spectrum analysis for non-classically damped linear system with multiple-support excitations", *Bull. Earthq. Eng.*, **6**(2), 261-284. https://doi.org/10.1007/s10518-007-9048-z.

Yu, R.F., Zhou, X.Y. and Yuan M.Q. (2012), "Dynamic response analysis of generally damped linear system with repeated eigenvalues", *Struct. Eng. Mech.*, **42**(4), 449-469. https://doi.org/10.12989/sem.2012.42.4.449.

Zhou, X.Y., Yu, R.F and Dong, D. (2004), "Complex mode superposition algorithm for seismic responses of non-classically damped linear MDOF system", *J. Earthq. Eng.*, **8**(4), 597-641. https://doi.org/10.1142/S1363246904001602.

PL

Appendix A

Using Eq. (15), we have,

$$\mathbf{\Phi}\dot{\mathbf{z}}(t) - \mathbf{\Phi}\mathbf{J}\,\mathbf{z}(t) = \mathbf{\Phi}\mathbf{a}^{-1}\mathbf{\Phi}^{\mathrm{T}}\mathbf{f}(t) \tag{A1}$$

From Eqs. (38)-(39), two equivalent expressions can be found for the velocity response: the first one is the derivative of the displacement response, i.e., $\dot{\mathbf{u}}(t) = \mathbf{\Phi}\dot{\mathbf{z}}(t)$, and the second one corresponds to the first half of the state vector $\mathbf{v}$, i.e., $\dot{\mathbf{u}}(t) = \mathbf{\Phi}\mathbf{J}\,\mathbf{z}(t)$. Considering any loading or time, $\mathbf{\Phi}\mathbf{a}^{-1}\mathbf{\Phi}^{\mathrm{T}}\mathbf{f}(t) = \mathbf{0}$ always holds. We then have,

$$\mathbf{\Phi}\mathbf{a}^{-1}\mathbf{\Phi}^{\mathrm{T}} = \mathbf{0} \tag{A2}$$

Pre-multiplying Eq. (6) by $\mathbf{\Psi}^{\mathrm{T}}$ and expanding it yields,

$$\mathbf{J}^{\mathrm{T}}\mathbf{\Phi}^{\mathrm{T}}\mathbf{M}\mathbf{\Phi} - \mathbf{\Phi}^{\mathrm{T}}\mathbf{K}\mathbf{\Phi}\mathbf{J}^{-1} = \mathbf{a} \tag{A3}$$

Pre-multiplying the above equation by $\mathbf{\Phi}\mathbf{a}^{-1}$ and recalling Eq. (15) yields,

$$\mathbf{\Phi}\mathbf{a}^{-1}\mathbf{J}^{\mathrm{T}}\mathbf{\Phi}^{\mathrm{T}}\mathbf{M} = \mathbf{I} \tag{A4}$$

Then,

$$\mathbf{M}^{-1} = \mathbf{\Phi}\mathbf{a}^{-1}\mathbf{J}^{\mathrm{T}}\mathbf{\Phi}^{\mathrm{T}} \tag{A5}$$

Similarly, post-multiplying Eq. (A3) by $\mathbf{a}^{-1}\mathbf{\Phi}^{\mathrm{T}}$ and recalling Eq. (15) yields,

$$-\mathbf{K}\mathbf{\Phi}\mathbf{J}^{-1}\mathbf{a}^{-1}\mathbf{\Phi}^{\mathrm{T}} = \mathbf{I} \tag{A6}$$

Then,

$$\mathbf{K}^{-1} = -\mathbf{\Phi}\mathbf{J}^{-1}\mathbf{a}^{-1}\mathbf{\Phi}^{\mathrm{T}} \tag{A7}$$

Appendix B

When the damping matrix in Eq. (3) is the form of Rayleigh damping, i.e., $\mathbf{C} = \alpha\mathbf{M} + \beta\mathbf{K}$, where α and β are proportionality constants, the system described in the state space still becomes defective if any modal damping ratio is critical. In such case, the eigenvalue problem in Eq. (6) can be transformed from the state space into the physical space and expressed as

$$\mathbf{K}\mathbf{\Phi} = -\mathbf{M}\mathbf{\Phi}(\mathbf{J}^2 + \alpha\mathbf{J})(\mathbf{I} + \beta\mathbf{J})^{-1} \tag{B1}$$

wherein $\mathbf{I}$ denotes an identity of order $2n$. The sizes of $\mathbf{\Phi}$ and $\mathbf{J}$ are $n \times 2n$ and $2n \times 2n$, respectively. Recalling the different features of critical and non-critical damping modes, it is convenient to expand Eq. (B1) for each individual mode.

For non-critical damping modes in pairs, the above equation can be expanded as,

$$\begin{cases} \mathbf{K}\boldsymbol{\phi}_i = -\dfrac{\lambda_i(\lambda_i + \alpha)}{1 + \beta\lambda_i}\mathbf{M}\boldsymbol{\phi}_i \\ \mathbf{K}\boldsymbol{\phi}_i^* = -\dfrac{\lambda_i^*(\lambda_i^* + \alpha)}{1 + \beta\lambda_i^*}\mathbf{M}\boldsymbol{\phi}_i^* \end{cases} \tag{B2}$$

For critical damping modes, even though $\mathbf{J}$ is not diagonal, similarly decoupled equations can be obtained due to the proportional performance of the damping matrix, namely,

$$\begin{cases} \mathbf{K}\boldsymbol{\phi}_r = \lambda_r^2\mathbf{M}\boldsymbol{\phi}_r \\ \mathbf{K}\boldsymbol{\phi}_r^* = \lambda_r^{*2}\mathbf{M}\boldsymbol{\phi}_r^* \end{cases} \tag{B3}$$

Obviously, both $\boldsymbol{\phi}_r$ and $\boldsymbol{\phi}_r^*$ satisfy the eigenvector equation, which is very different from that in non-classically damped systems.

Normalizing $\boldsymbol{\phi}_i$ and $\boldsymbol{\phi}_i^*$ with respect to the mass matrix as well as the undamped mode $\boldsymbol{\phi}_i^{\mathrm{R}}$, the following relationship can be obtained as,

$$\boldsymbol{\phi}_i^{\mathrm{R}} = \boldsymbol{\phi}_i = \boldsymbol{\phi}_i^* \tag{B4}$$

Although $\boldsymbol{\phi}_i = \boldsymbol{\phi}_i^*$, the corresponding eigenvectors in the state space, i.e., $\boldsymbol{\psi}_i^{\mathrm{T}} = \left[\lambda_i(\boldsymbol{\phi}_i^{\mathrm{R}})^{\mathrm{T}}, (\boldsymbol{\phi}_i^{\mathrm{R}})^{\mathrm{T}}\right]$ and $\boldsymbol{\psi}_i^{*\mathrm{T}} = \left[\lambda_i^*(\boldsymbol{\phi}_i^{\mathrm{R}})^{\mathrm{T}}, (\boldsymbol{\phi}_i^{\mathrm{R}})^{\mathrm{T}}\right]$, are linearly independent. However, if $\lambda_r = \lambda_r^* = -\omega_r$, $\boldsymbol{\psi}_r$ and $\boldsymbol{\psi}_r^*$ are linearly dependent such that the classically damped system with critical modal damping described in the state space are defective. In this situation, the proposed eigenvectors, i.e., $\boldsymbol{\psi}_r^{\mathrm{T}} = [\lambda_r(\boldsymbol{\phi}_r^{\mathrm{R}})^{\mathrm{T}}, (\boldsymbol{\phi}_r^{\mathrm{R}})^{\mathrm{T}}]$, $\boldsymbol{\psi}_r^{*\mathrm{T}} = [(1 + \lambda_r)(\boldsymbol{\phi}_r^{\mathrm{R}})^{\mathrm{T}}, (\boldsymbol{\phi}_r^{\mathrm{R}})^{\mathrm{T}}]$, should be used, which can construct a complete set of vector bases for the state space in conjunction with $\boldsymbol{\psi}_i$ and $\boldsymbol{\psi}_i^*$.

When the damping matrix in Eq. (3) is the form of Rayleigh damping, the eigenvalue can be written as,

$$\lambda_i, \lambda_i^* = -\xi_i\omega_i \pm \omega_i\sqrt{\xi_i^2 - 1} \tag{B5}$$

which is different from Eq. (4), since ω_i and ξ_i herein are the i-th undamped natural frequency and the modal damping ratio of the classically damped system.

Utilizing the obtained relationships between $\boldsymbol{\phi}_i^{\mathrm{R}}$ and $\boldsymbol{\psi}_i$ or $\boldsymbol{\psi}_i^*$ as well as ω_i and λ_i or λ_i^*, the factors required in the complex mode superposition approach can be given by,

$$\begin{cases} \eta_i = \dfrac{\gamma_i}{2\omega_i\sqrt{\xi_i^2 - 1}}, \eta_i^* = -\dfrac{\gamma_i}{2\omega_i\sqrt{\xi_i^2 - 1}} & \xi_i \neq 1 \\ \eta_i = -\gamma_i, \qquad \eta_i^* = \gamma_i & \xi_i = 1 \end{cases} \tag{B6}$$

wherein $\gamma_i = (\boldsymbol{\phi}_i^{\mathrm{R}})^{\mathrm{T}}\mathbf{s} / \left[(\boldsymbol{\phi}_i^{\mathrm{R}})^{\mathrm{T}}\mathbf{M}\boldsymbol{\phi}_i^{\mathrm{R}}\right]$ refers to the conventional modal participation coefficient. These factors above can yield $\boldsymbol{\rho}_i^d = \mathbf{0}, \boldsymbol{\varphi}_i^d = \gamma_i\boldsymbol{\phi}_i^{\mathrm{R}}$. The conventional mode superposition method and MAM are then recovered.